



HAL
open science

Eco-Friendly Production of Hyper-Cross-Linked Polymers Using Mechanosynthesis and Bioresources: A Critical Review

Antonio M. Borrero-López, Alain Celzard, Vanessa Fierro

► **To cite this version:**

Antonio M. Borrero-López, Alain Celzard, Vanessa Fierro. Eco-Friendly Production of Hyper-Cross-Linked Polymers Using Mechanosynthesis and Bioresources: A Critical Review. ACS Sustainable Chemistry & Engineering, 2022, 10 (49), pp.16090-16112. 10.1021/acssuschemeng.2c04954 . hal-04146315

HAL Id: hal-04146315

<https://hal.univ-lorraine.fr/hal-04146315v1>

Submitted on 29 Jun 2023

HAL is a multi-disciplinary open access archive for the deposit and dissemination of scientific research documents, whether they are published or not. The documents may come from teaching and research institutions in France or abroad, or from public or private research centers.

L'archive ouverte pluridisciplinaire **HAL**, est destinée au dépôt et à la diffusion de documents scientifiques de niveau recherche, publiés ou non, émanant des établissements d'enseignement et de recherche français ou étrangers, des laboratoires publics ou privés.

Eco-friendly production of hyper-crosslinked polymers using mechanosynthesis and bioresources: a critical review

Antonio M. Borrero-López^{†,‡,*}, Alain Celzard[†], Vanessa Fierro^{†,*}

[†] *Université de Lorraine, CNRS, IJL, F-88000 Epinal, France*

[‡] *Pro2TecS – Chemical Process and Product Technology Research Centre. Dept. Chemical Engineering, ETSI. Campus de “El Carmen”. Universidad de Huelva. 21071 Huelva. Spain*

* Corresponding authors: Antonio M. Borrero-López: antonio.borrero-lopez@univ-lorraine.fr; +34959218201; ENSTIB, 27 rue Philippe Séguin, BP 21042, 88051 Épinal cedex 9, France, Vanessa Fierro: vanessa.fierro@univ-lorraine.fr; ENSTIB, 27 rue Philippe Séguin, BP 21042, 88051 Épinal cedex 9, France

Abstract

Hyper-crosslinked polymers (HCPs) are receiving great attention due to their high specific surface area, allowing them to offer high performance in many different applications. However, most of the time, their synthesis requires hazardous and time-consuming protocols, making their implementation and scaling up difficult. To overcome this problem, a relatively old technology such as mechanosynthesis (MS) has gained renewed interest as a greener and faster technology to produce HCPs, which involves much lower energy consumption during the reaction process. In this review, the latest advances on the performance of HCPs based on MS protocols are compiled and analysed, subdivided into those based on Friedel-Crafts alkylation, Scholl coupling reactions and other less common procedures. An analysis of MS versus solvent-based protocols regarding the twelve principles of green chemistry is also reported, as well as a section including a summary of the most recent applications of HCPs. Finally, the use of bio-based precursors for the formulation of HCPs is discussed, thus pooling knowledge for a greener, faster and more widely applicable future development of HCPs.

Keywords: Mechanosynthesis; bioresources; hyper-crosslinked polymers; porous materials; green chemistry

List of abbreviations

Ani - Aniline

A_{BET} – Surface area based on Brunauer, Emmett and Teller theory

Ben – Benzene

BCB – 4,4'-Bis(chloromethyl)-1,1'-biphenyl

BET – Brunauer, Emmett and Teller

Biph – Biphenyl

BPA – Bisphenol A

BPAF – Bisphenol AF

BPF – Bisphenol F

BPS – Bisphenol S

COF – Covalent organic framework

CP MAS – Cross-polarized magic angle spinning spectrometry

DBU – 1,8-Diazabicyclo[5.4.0]undec-7-ene

DCE – Dichloroethane

DCM – Dichloromethane

DMF – Dimethylformamide

EtOH – Ethanol

FC – Friedel-Crafts

FC_{sb} – Solvent-based Friedel-Crafts

FDA – Formaldehyde dimethyl acetal or dimethoxymethane

FTIR – Fourier-transform infrared

HCP – Hyper-crosslinked polymer

Im – Imidazole

LAG – Liquid assisted grinding

MB – Methylene blue chloride

MeOH – Methanol

MeCN – Acetonitrile

MS – Mechanosynthesis

NMR – Nuclear magnetic resonance

PEG – Polyethylene glycol

PMEPV – Poly(2-methoxy-5-2'-ethylhexyloxy phenylene vinylene)

Py – Pyrrole

Pyr – Pyridine

Pros – 1,3-Propanesultone

PSD - Pore size distribution

PTFE – Polytetrafluoroethylene (Teflon™)

RhoB – Rhodamine B

SC – Scholl coupling

SO – Safranin O

SC_{sb} – Solvent-based Scholl coupling

SS – Stainless steel

t-BuOK – Potassium tert-butylate

TEOA – Triethanolamine

THF – Tetrahydrofuran

TMB – Tetramethylbenzene

Tos – 1,3-*p*-Toluenesulfonic acid

TPB – Triphenylbenzene

TTP – 3,3,3',3'-Tetramethyl-2,2',3,3'-tetrahydro-1,1'-pirobi[indene]-6,6'-diol

Introduction

Hyper-crosslinked polymers (HCPs) represent, as the name suggests, a class of entangled polymers where the high level of crosslinking results in materials with porosity typically below 2 nm, *i.e.*, corresponding to micropores. Their structure is stable and rigid due to both the nature of the linkages and the extensive entanglement. They are therefore high-surface area polymers.¹ These HCPs have attracted a lot of attention in the last decades and have proven to be valuable in areas such as heterogeneous catalysts,²⁻⁴ chromatographic separation,¹ gas adsorption⁵ (*i.e.*, hydrogen,⁶ CO₂,^{4,7-9} volatile organic compounds¹⁰⁻¹² and vapours¹³), removal of heavy metal ions^{11,14} and hazardous dyes¹¹, and drug delivery, among others.¹

Usually, HCPs are synthesised by Friedel-Crafts (FC) and Scholl coupling (SC) reactions, which involve long reaction times, moderate temperatures (about 40-110 °C) and involve hazards from the solvents used.^{1,2,5,6,10} Both types of synthesis protocols are based on the swelling of monomers and the formation of an entangled polymer structure, which is achieved by selecting a compatible solvent that can be introduced into the polymer matrix. Another common feature is that both are catalysed by Lewis acids, such as FeCl₃, AlCl₃, SnCl₄, etc. Thus, the main difference lies in the structure generated, as an external crosslinker causes entanglement in the FC protocol, whereas for the SC procedure, the entanglement is based on the reaction between the monomer molecules themselves.¹⁵ Although valuable results have been obtained in many different fields for these various HCPs, as mentioned above, the risk associated with the processing protocol and its usual long duration require that research be directed towards more environmentally friendly and faster protocols.

For these reasons, the present review deals with mechanosynthesis (MS), a relatively old technology that has recently regained attention due to interesting new approaches. It was first defined by Gerhard Heinicke, who established in 1984 that “*mechanochemistry is that branch of chemistry which is concerned with the chemical and physical changes of solids which are induced by the action*

of mechanical influences".¹⁶ It consists of a very simple process, where a ball mill is used as a reactor, usually a cylindrical bowl with a rounded edge, made of different materials, and which is filled with spherical balls of known diameters, usually of the same material as the bowl. In this environment, the materials to be reacted are added, and the bowl is closed and stirred for a set period, with or without pauses. The total time for MS is generally much shorter than for conventional FC or SC reaction routes (reaction times of a few minutes to a few hours for MS, compared to 12 h to several days for FC and SC).^{15,17,18} Grinding and high-energy collisions cause reactions between the different precursors, generally at room temperature and without the need for additional solvent, which highlights the greener and more efficient approach of the method and significantly reduces the overall energy spent during the entire procedure. In this sense, it is also worth mentioning that it is not necessary to have a single-phase and homogenous reaction medium to obtain high-surface area and multifunctional products by MS, which is another key point that emphasises the easier use of this technique compared to common solvent-based protocols. Nevertheless, there are many studies where solvents of different types are added, a method known as liquid-assisted grinding (LAG).^{15,19,20}

Due to the above-mentioned features, MS can also be considered a very safe protocol, as the reactions take place in a sealed environment, thus with little possibility of leakage. In addition, a maximum volume is usually specified by the manufacturer, to avoid temperatures and pressures that could lead to equipment failure and/or explosions. On the other hand, in order to gain control over the reactions involved, *ex situ* techniques have been generally used, which have allowed the different states of the reactions to be monitored. However, more recently, some *in situ* devices have also been designed. The simplest ones are able to control temperature and/or pressure within the equipment, but X-ray diffraction measurements and Raman spectroscopy have also been performed.²¹ In this way, not only can the reaction be operated more safely, but the continuous formation of different products can also be monitored, and the results have shed light on how certain reactions are conducted in this scenario.

Depending on the way the movement of the bowl is performed, two different types of MS grinding are encountered in the literature. On the one hand, planetary mills, as the name suggests, consist of a grinding bowl, containing balls and the material to be processed, arranged eccentrically on a so-called sun-wheel whose direction of movement is opposite to that of the bowl. On the other hand, mixing mills (also known as shaking or vibrating mills), have their bowl oscillating along the same axis.^{17,22,23} The mixing speed of the two types of MS motion is usually measured in rpm and Hz, respectively (see schematic representation of the two kinds of movements in Fig. 1A).

During MS, reactions take place due to the high-energy impacts caused by the grinding balls and occur at room temperature.^{13,15,24–26} In the literature, many different materials have been tested for grinding, providing different impact energies, namely polytetrafluoroethylene (PTFE), silicon nitride (Si_3N_4), zirconium oxide (ZrO_2), stainless steel (SS) and tungsten carbide (WC). The impact energy indeed depends on the density of the material, so the higher the density, the higher the impact, and therefore the higher the energy provided. From the lowest to the highest density, PTFE (2.2 g/cm^3), Si_3N_4 (3.17 g/cm^3), ZrO_2 (5.7 g/cm^3), SS (7.9 g/cm^3) and WC (14.9 g/cm^3) are available.¹⁵ The most common material used in literature is ZrO_2 , as some authors have suggested that excessive energy inputs due to high densities produce excessive abrasion of the MS grinding components (both balls and bowl), but also their chlorination (metal chlorides being frequently used as Lewis acids to catalyse the synthesis of HCPs).²⁴ The possible catalytic effect of metals must also be considered. Thus, a careful choice of grinding material can help to avoid the addition of a catalyst, as in the study by Cook et al.,²⁷ where a copper-based grinding material was used to directly catalyse the azide-alkyne cycloaddition. Another example can be found in the work of Haley et al.,²⁸ where they used cylindrical nickel pellets both as a catalyst and to produce the high-energy impacts, instead of the usual spherical balls. On the other hand, the reaction time is also known to be a crucial parameter in MS. In general, low times lead to low yields, while too high reaction times also lead to further deterioration of the HCP properties. Nevertheless, each precursor combined with the other MS

conditions selected (grinding material, ball size and number, etc.) has its own optimal reaction time.^{15,17}

Despite all the advantages mentioned, the use of MS for the production of HCPs is not widespread. In the present review, we discuss the latest achievements in the preparation of HCPs by Friedel-Crafts and Scholl coupling reactions following MS routes, as well as less common procedures. The main MS parameters as well as precursors, catalysts, crosslinkers and other alternative additional compounds, such as solvents and/or bulking agents, *i.e.*, inert additives enabling control of the reaction scale, that have been tested in the literature are analysed here.

Mechanosynthesis of hyper-crosslinked polymers

Friedel-Crafts (FC) approach

The common solvent-based Friedel-Crafts (FC) approach has led to a wide range of useful formulations, based on which the surface areas of the resulting materials could reach very high values, e.g., 1390 m²/g using benzene as a precursor, or 1470 m²/g using tetraphenylmethane, for instance.²⁹ In order to provide a general description of the FC reaction and the MS procedure, Fig. 1B includes a visual description of an MS reaction providing a benzene-based HCP by using dimethoxymethane, also called formaldehyde dimethyl acetal (FDA), as a crosslinker, together with some other examples of the main precursors, catalysts and crosslinkers present in literature.

Lee et al.¹⁵ tested six different aromatic compounds, namely benzene, pyrrole, aniline, biphenyl, triphenylbenzene and tetramethylbenzene (see Fig. 1C), and reported reaction times of only 10 s to produce benzene-based microporous HCPs. Different MS variables were studied for the production of benzene-based HCPs using FeCl₃ as a catalyst, such as reaction time, catalyst/monomer ratio (see Fig. 1D) and grinding speed. MS of benzene for 5 min using a FeCl₃/benzene molar ratio of 6 and a rotation speed of 800 rpm resulted in the highest BET area ($A_{\text{BET}} = 626 \text{ m}^2/\text{g}$) and porosity. An increase in reaction time resulted in a lower surface area, probably due to the high energy of the MS,

leading to the breakage of the C-C bonds in the polymer structure. Similarly, an increase in the FeCl₃/monomer ratio or the amount of crosslinker also gave lower surface areas. This finding is explained by the blocking of all available benzene sites, which can no longer polymerise, leading to a low level of polymerisation, and by the terminal groups of the single-bonded crosslinker, producing pore blocking. Tetraphenylbenzene was the precursor giving rise to the HCP with the highest BET area (784 m²/g).

Four other different aromatic compounds, such as stilbene, tetraphenylethylene, naphthalene and toluene, as well as biphenyl, were also used as HCP precursors by MS.³⁰ The maximum BET area obtained in this case was 556 m²/g, based on the biphenyl precursor. The thermal stability of the HCPs was also measured and they were found to be stable up to over 200°C. Two different thermal events were observed at high temperature, always leading to residues above 60 wt.%, with the biphenyl-based HCP showing the highest thermal stability. The different polymers were tested for *p*-nitrophenol removal, obtaining up to more than 150 mg/g of *p*-nitrophenol adsorbed in the HCP. The A_{BET} was also measured after the adsorption tests and negligible changes were observed, demonstrating the ability of HCPs to maintain their structural integrity. As can be observed, lower surface areas are generally obtained by using MS compared to solvent-based reactions, which implies that more knowledge is still needed to achieve such high values.

Using 1,3,5-triphenylbenzene as a precursor and two different types of organochloride crosslinkers, namely dichloromethane (DCM) and chloroform, Krusenbaum et al.¹⁸ carried out an extensive study of several crucial parameters for producing HCPs. Thus, the crosslinker/monomer ratio and MS reaction time were varied (see Fig. 1E). The reaction was confirmed by ¹H → ¹³C cross-polarized magic angle spinning spectrometry (CP MAS), as well as by FTIR spectroscopy. The thermal stability of the HCPs was significantly different from that obtained using FDA as a crosslinker. In this case, the samples were able to hold temperatures up to 400°C, however, residues of no more than 10 wt.% were obtained, evidencing a much lower final thermal stability when using DCM or

chloroform. In the case of DCM as a crosslinker, increasing the crosslinker/monomer molar ratio from 1:1 to 15:1 always resulted in an increase in A_{BET} , with values above $1600 \text{ m}^2/\text{g}$ for the highest ones. Although a higher degree of crosslinking could initially be expected by using chloroform instead of DCM due to its higher functionality, similar crosslinker/monomer ratios only provided a maximum A_{BET} below $1400 \text{ m}^2/\text{g}$. However, ratios around 2-4 already provided an A_{BET} above $1000 \text{ m}^2/\text{g}$, which was not achieved using DCM. An increase in reaction time, studied in the range of 5-120 min again led to higher A_{BET} values for DCM-based HCPs, while with the use of chloroform, a maximum was found at 60 min. The frequency of the vibrating mill was also evaluated (Fig. 1E), again giving a maximum, in this case at 30 Hz, while either an increase or a decrease of it led to lower A_{BET} values for all organochlorine crosslinkers tested. These maxima, again, are consistent with the general assumption that too much energy input can lead to lower surface areas due to the collapse of the polymer structure. Analysis of the pore size distribution (PSD) revealed some similarity between the effects of the two crosslinkers on the pore texture, with an average pore diameter of less than 2 nm.

On the other hand, heteroatoms have also been introduced in order to provide HCPs with improved properties in different application areas. Thus, N-doped HCPs were synthesised using cyanuric chloride as the nitrogen source and different aromatic building blocks as monomers, namely carbazole, anthracene, triphenylbenzene, tetraphenylmethane and naphthalene (see Fig. 1F).²⁶ Under similar characterisation conditions to those used by Lee et al.¹⁵ (argon adsorption at $-186 \text{ }^\circ\text{C}$), the tetraphenylbenzene-based HCP exhibited the highest surface area, this time reaching $590 \text{ m}^2/\text{g}$ when using tungsten carbide as the bowl and ball material and grinding for 60 min. Different grinding times were studied using carbazole as a precursor and a plateau value in A_{BET} of around $780 \text{ m}^2/\text{g}$ based on N_2 adsorption was observed for grinding times above 15 min (see Fig. 1G). Using carbazole as HCP precursor, a PSD with very narrow pores was obtained, with two peaks at 0.5 and 1 nm. The

reaction was monitored by ^{13}C Nuclear Magnetic Resonance (NMR) and Heteronuclear Multiple Bond Correlation, showing the presence of carbazole oligomers after 10 min.

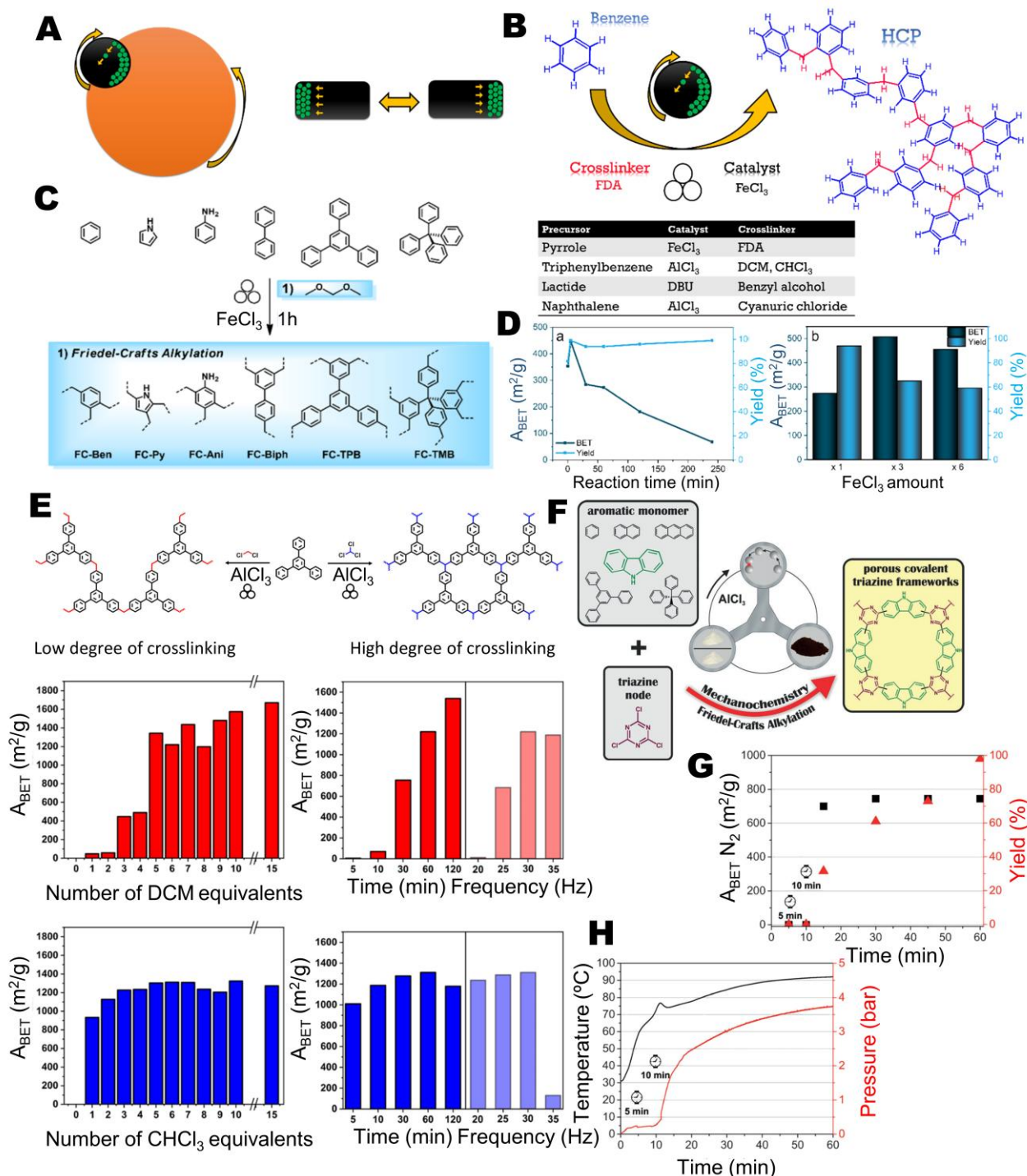


Figure 1. A) Schematic motion of planetary ball milling (left) and mixer milling (right). B) Friedel-Crafts reaction scheme of the formation of a HCP by MS from benzene and FDA (crosslinks are marked in red). Table: other precursors, catalysts and crosslinkers that have been used. C) Synthesis of HCPs by FC alkylation.¹⁵ D) Effect of (a) milling time and (b) amount of FeCl_3 on the BET area and yield of a benzene-based HCP.¹⁵ Reprinted with permission from Lee JSM, Kurihara T, Horike S. Five-Minute Mechanochemistry of Hypercrosslinked Microporous Polymers. *Chem Mater* 2020;32:7694–702. Copyright 2020 American Chemical Society. E) (top) Schematic overview of the mechanochemical Friedel-Crafts alkylation of 1,3,5-triphenylbenzene with DCM (left; red) and with CHCl_3 (right; blue) as crosslinking agents; (bottom) A_{BET} of HCPs as a function of whether DCM (red) or CHCl_3 (blue) was selected (left), and as a function of milling time (right, dark) and milling frequency (right; light) for DCM (red) and CHCl_3 (blue).¹⁸ Adapted with

permission from Krusenbaum A, Geisler J, Joel F, Kraus L, Grätz S, Valentin M, et al. The mechanochemical Friedel-Crafts polymerization as a solvent-free cross-linking approach toward microporous polymers. *J Polym Sci* 2022;60:62–71. Copyright 2022 Wiley. . F) Mechanochemical synthesis of porous covalent triazine frameworks by Friedel–Crafts alkylation of different aromatic monomers with cyanuric chloride.²⁶ G) Evolution of A_{BET} measured by nitrogen adsorption and yield as a function of reaction time, as well as H) in-situ analysis of temperature and pressure in the milling jar, for carbazole-based HCPs.²⁶ Reprinted with permission from Troschke E, Grätz S, Lübken T, Borchardt L. Mechanochemical Friedel-Crafts Alkylation-A Sustainable Pathway Towards Porous Organic Polymers. *Angew Chemie* 2017;129:6963–7. Copyright 2017 Wiley.

The corresponding temperature and pressure profiles were also reported, and they showed a substantial increase with grinding time, reaching over 90 °C and up to 4 bar at 60 min of grinding (see Fig. 1H). In the latter study, the use of different bulking agents to control the reaction was evaluated, with LiCl producing the highest A_{BET} , 620 m²/g, followed by ZnCl₂, NaCl and KCl, with 570, 560 and 485 m²/g, respectively.²⁶

Scholl coupling (SC) approach

Using Scholl coupling (SC) approach, a wide variety of HCPs has also been synthesized, with an A_{BET} of 1421 m²/g, obtained by using triphenylbenzene and pyrrole, 1337 m²/g by selecting pitch instead, or 1119 m²/g by using triphenylamine.²⁹ Fig. 2A shows the schematic representation of HCPs derived from SC reactions. As can be seen, no crosslinker is now added, and the bonds are obtained directly between the monomer molecules themselves, illustrated by the benzene-benzene bonds.

Lee et al.¹⁵ tested the same four different aromatic compounds as mentioned above in SC reactions, namely pyrrole, biphenyl, triphenylbenzene and tetramethylbenzene. Depending on the precursor, the HCPs obtained exhibited higher (tetramethylbenzene), very similar (pyrrole) or lower (triphenylbenzene and biphenyl) A_{BET} than those produced following the FC approach, again emphasising the crucial importance of the precursor for MS protocols. In order to extend the study, liquid-assisted grinding (LAG), using a wide range of solvents, was also tested following the SC protocol. Thus, polar protic solvents (such as methanol, ethanol, water, formic and acetic acid), polar aprotic solvents (such as N,N-dimethylformamide (DMF), ethyl acetate and pyridine), and nonpolar solvents (such as n-hexane, cyclohexane and dichloromethane (DCM)) were used. Although no

direct correlation between porosity and solvent properties could be obtained, generally higher A_{BET} values were reported using solvents compared to the non-LAG protocol. Another interesting key point worth mentioning is that some of these solvents (*e.g.* MeOH and water) could not produce HCPs by typical Friedel-Crafts procedures.

Grätz et al.¹³ developed HCPs following MS reactions by using 4,4'-bis(chloromethyl)-1,1'-biphenyl (BCB) as precursor and FeCl_3 as catalyst. Once again, the authors pointed out that excessive energy supplied to the system led to lower A_{BET} due to the partial degradation of the structure, but this time this occurred by increasing the rotational speed from 500 to 800 rpm. However, low rotational speeds (200 rpm) resulted in an even lower A_{BET} . In this sense, a maximum was again observed, in agreement with the work of Krusenbaum et al.¹⁸ The highest values of A_{BET} were obtained by the LAG protocols. For this, different solvents were tested, namely diethyl ether, DCM, chloroform, tetrahydrofuran, ethanol, methanol, ethyl acetate and isopropanol. Optimal values were obtained using diethyl ether, for which an A_{BET} of $1720 \text{ m}^2/\text{g}$ and pore volumes of $1.55 \text{ cm}^3/\text{g}$ were achieved (after activation at $80 \text{ }^\circ\text{C}$ for 24h under vacuum, improving on what was obtained without the presence of solvent ($850 \text{ m}^2/\text{g}$)). This time, a trend was indeed found, as the lower the boiling point of the solvent, the higher the A_{BET} obtained. This may be related to the fact that solvents vaporise in the mixture, and that vapour is more efficient than liquid as a pore generator. These HCPs have been studied as adsorbents for benzene and cyclohexane vapours, with excellent results (uptakes of over 1000 and $600 \text{ cm}^3/\text{g}$, respectively, at a relative vapour pressure of 0.95).

In another work, 1,3,5-triphenylbenzene was once more used as the main precursor, but tetraphenylmethane, tetraphenyl-ethylene, 2,4,6-triphenylbenzene-1,3,5-triazine, triphenylamine and 1,3,5-tris(N-carbazolyl)benzene were also tested. A very comprehensive study of MS conditions was carried out, where Krusenbaum et al.¹⁷ evaluated many different parameters, such as grinding material, reaction time, liquid assistance, ball size, initial temperature of the mixture and type of grinding (see Fig. 2B). HCP formation was checked by CP MAS, FTIR, thermogravimetric analysis

and X-ray powder diffraction. In the absence of crosslinkers, the thermal stability was quite high, with no significant change up to 400°C, and with a weight loss of about 10 wt.% at 550°C. Optimal A_{BET} values for 1,3,5-triphenylbenzene were again obtained at very low grinding times of 5 min, in good agreement with Lee et al.¹⁵ Comparing the different precursors, 1,3,5-tris(N-carbazolyl)benzene was able to produce HCPs with up to 3 times higher A_{BET} than HCPs based on 1,3,5-triphenylbenzene under the same experimental conditions. LAG was also evaluated. Many different solvents were used, with halogenated solvents showing the highest A_{BET} values for the corresponding HCPs. For the first time, the initial MS temperature was modified and the resulting HCPs were evaluated, with 100 °C being the optimal temperature found.

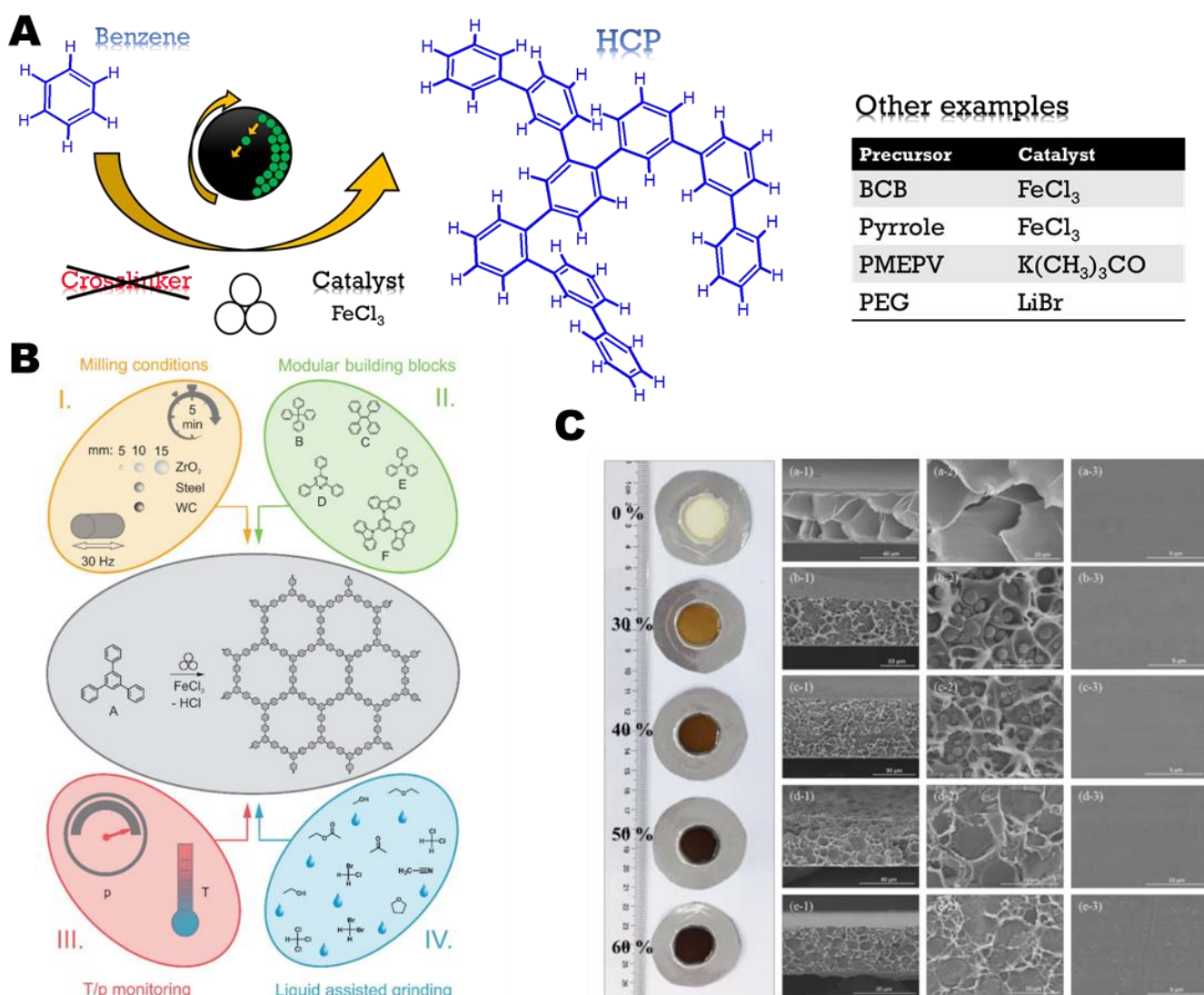


Figure 2. A) Schematic of the Scholl coupling reaction for the formation of a HCP by MS, including the main precursors and catalysts involved (benzene was used as a model compound for the HCP structure). B) Schematic overview of the variation of the Scholl reaction parameters. The middle (grey) part shows the standard reaction. For this, monomer A (1,3,5- triphenylbenzene) is used. I. Systematic variation of milling parameters (yellow), such as time, frequency, and size and density of the milling material. II. Variation of the monomers used for the Scholl reaction (green). For the reaction, monomers B (tetraphenylmethane), C (tetraphenyl- ethylene), D (2,4,6-triphenylbenzene-1,3,5-triazine), E (triphenyl- amine) and F (1,3,5-tris(N-carbazolyl)benzene) were used. III. Temperature variation during the reaction (pink). IV. Scholl reaction with liquid-assisted grinding (LAG, blue).¹⁷ Reprinted from Ref.¹⁷ with permission from the Royal Society of Chemistry. C) Photos (left) of TTP-based HCP/polyimide films with TTP-based HCP content ranging from 0 to 60 wt.%; SEM images (right) of (1, 2) cross-section and (3) top surface of TTP-based HCP/polyimide membranes: (a) 0 wt.%; (b) 30 wt.%; (c) 40 wt.%; (d) 50 wt.%; (e) 60 wt.%. Scale bars: a-1 and d-1 (40 μm); c-1 and e-1 (30 μm); b-1, a-2, d-2, e-2 and d-3 (10 μm); b-2, c-2, a-3, b-3, c-3 and e-3 (5 μm).³¹ Reprinted with permission from Zhu X, Hua Y, Tian C, Abney CW, Zhang P, Jin T, et al. Accelerating Membrane-based CO₂ Separation by Soluble Nanoporous Polymer Networks Produced by Mechanochemical Oxidative Coupling. *Angew Chemie – Int Ed* 2018;57:2816–21. Copyright 2018 Wiley.

Zhu et al.³² also developed carbazole-based HCPs using MS. The A_{BET} and pore volume of the optimal HCP were 707 m²/g and 0.45 cm³/g, respectively. Thus, the A_{BET} was enhanced by almost 50% compared to the traditional solvent-based process. In another study, Zhu et al.³¹ developed HCPs, which can be used for membrane casting for CO₂/CH₄ separation, by MS of 3,3,3',3'-

tetramethyl-2,2',3,3'-tetrahydro-1,1'-pirobi[indene]-6,6'-diol (TTP), which produced HCPs with A_{BET} above 800 m²/g. Moreover, this HCP showed excellent solubility in solvents such as THF, ethyl acetate and dimethylformamide. In fact, the significant changes in A_{BET} after dissolution suggest that swelling in different solvents may account for this parameter. Another interesting feature of this HCP is that, when irradiated under UV, it emits at a maximum wavelength of around 470 nm, suggesting a conjugated architecture. A summary of membranes characterisation is included in Fig. 2C, where it can be seen that concentrations as high as 60% of HCP can be added as fillers without altering the apparent visual homogeneity of the membrane. In fact, the SEM images showed increased uniformity as the filler content increased. Solvent-based reactions have generally resulted in higher surface areas than those obtained with MS, which again requires a deeper understanding of the phenomena that occur during both types of synthesis.²⁹

Other mechanosynthesis approaches

Grätz et al.³³ produced HCPs by the Suzuki cross-coupling reaction by subjecting 3,5-dibromophenylboronic acid and other compounds to MS with palladium acetate and potassium carbonate, both acting as catalysts, thus obtaining 3D mesoporous networks. Although A_{BET} was not measured in this study, polymerisation took place and was maintained up to degrees of polymerisation (defined as the number of monomers forming part of the polymer chain) of 164 after 30 minutes of grinding. Fig. 3A shows the precursors (1,3,5-tribromobenzene, 1,4-dibromobenzene, 1,4-dichlorobenzene, 1,4-diiodobenzene 1,4-phenyldiboronic acid, 4-bromophenylboronic acid, 3,5-dibromophenylboronic acid), the catalysts ($\text{Pd}(\text{OAc})_2$, K_2CO_3), the different grinding materials tested (Si_3N_4 , ZrO_2 , SS and WC), and the products obtained. The highest degrees of polymerisation were obtained for Si_3N_4 , significantly exceeding the values obtained using ZrO_2 , SS and WC (see Fig 3B). Thermogravimetric analysis showed very good thermal stabilities, depending on the reaction time. Thus, some mass loss at about 400°C took place for the sample synthesized at 30 min reaction time, while for the 120 min sample, the thermal event at this temperature was much lower, finally leading

to a residue about 10 wt.% higher (50 wt.%). By FTIR, significant changes could also be observed during HCP formation, mainly due to the disappearance of boron-oxygen and boron-carbon bond and the increase of aromatic rings.

Casco et al.²⁵ used MS to synthesise porous materials by mixing hexachlorobenzene, C₆Cl₆, and calcium carbide, CaC₂, at different ratios and using different grinding times. Maximum A_{BET} values of 915 m²/g were obtained for a CaC₂/C₆Cl₆ ratio of 5.1:1 and 120 min of grinding. However, these materials cannot be considered as HCPs but as carbonaceous materials, as carbon contents as high as 71-90 wt.% with predominant sp² hybridisation were obtained (see overview of the process and results in Fig. 3C). By the way, the electrical conductivity of the resultant materials ranged from 2.2 to 40.7 S/cm, and their A_{BET} from 120 to 915 m²/g. The increase in A_{BET} decreased the electrical conductivity although the values were similar to those of commercial activated carbons (between 1 and 100 S/cm).^{25,34}

Porous conjugated HCPs were also obtained by Chen et al.³⁵ by combining 1,2,4,5-tetrabromobenzene as a monomer and Mg acting as a dehalogenation agent (see summary of the HCP formation protocol in Fig. 3D). The maximum pore volume was 0.53 cm³/g, and A_{BET} reached 360 m²/g, based on an optimum molar ratio of monomer to Mg of 1:4. The change in PSD in the 1:4 ratio test was also very significant, as the distribution changed dramatically in mesopores of about 10 nm, while micro- and macropores were present together in the PSD of the 1:16 sample synthesized at 3 h. In contrast to the results of Lee et al.,¹⁵ MS reaction times of 3 h were required to achieve effective C-C bonding, again emphasising the importance of the monomer and the choice of MS conditions. However, an increase in reaction time to 5 h resulted in structural collapse due to a loss of micropores, which is consistent with achieving a maximum A_{BET} in the reaction time profile, as observed in previous studies.^{13,18} Other aromatic halides were tested and their reactivity was similarly evaluated, as shown in Fig. 3E. The resulting HCPs showed excellent performance as anodes for lithium batteries, with close results in cyclic voltammetry at low potentials (high

reversibility in the range 0.05-0.65 V vs Li/Li⁺) and significantly higher capacities (about 1000 mAh/g, compared to 372 mAh/g for graphite).³⁵

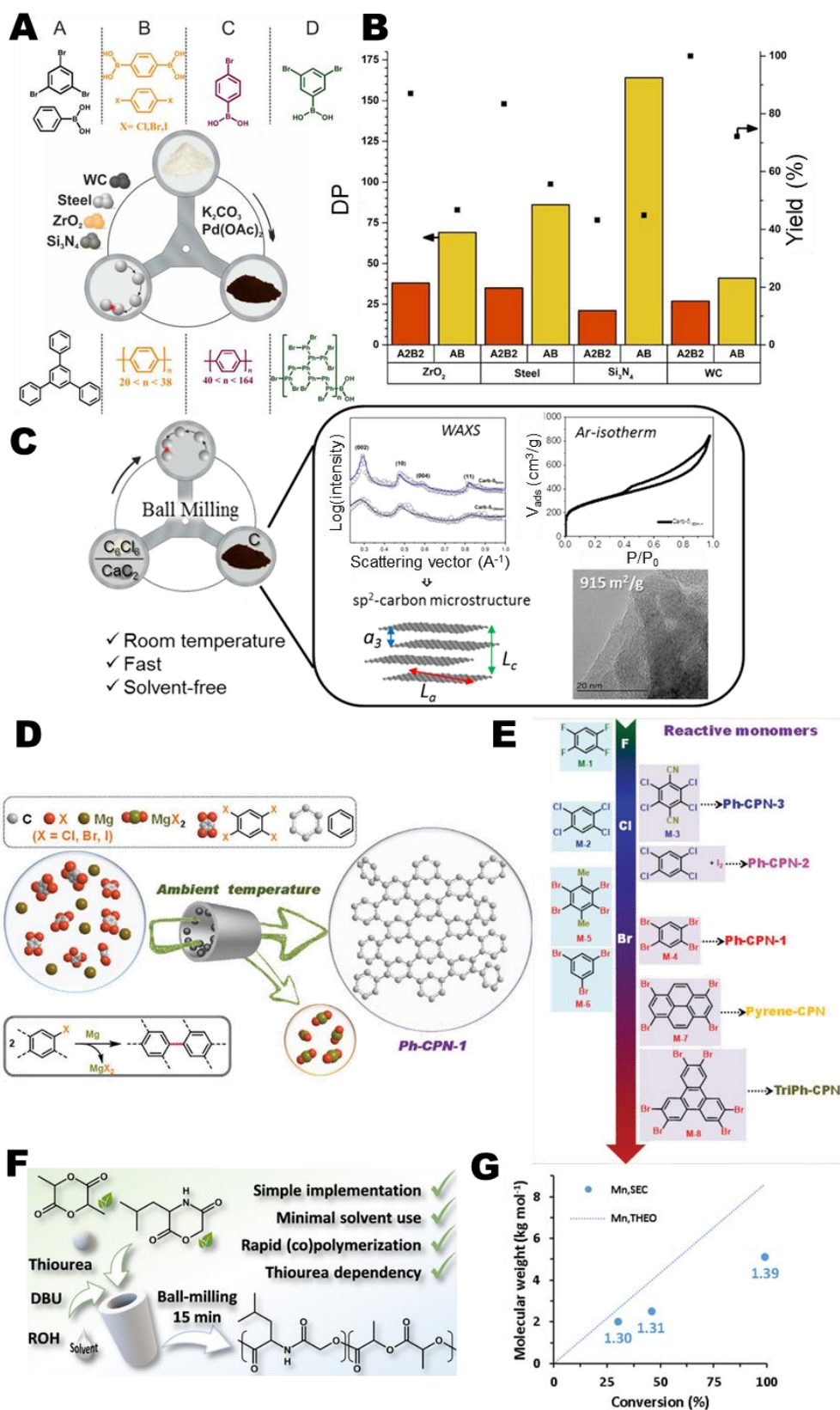


Figure 3. A) Schematic of the Suzuki cross-coupling reaction of different systems conducted in a planetary ball mill.³³ B) Comparison of four different milling materials for the A2B2 and AB approach, including the degree of polymerisation (DP) (bar chart) and yield (dots) (A2B2: polymer based on 1,4-Dibromobenzene and 1,4-Phenyldiboronic acid; AB: polymer based on 4-Bromophenylboronic acid).³³ Reproduced from Ref.³³ with permission from the Royal Society of Chemistry. C) Overview of the MS procedure and the main results of the study of Casco et al.²⁵ Reprinted from Carbon, 139, Casco ME, Badaczewski F, Grätz S, Tolosa A, Presser V, Smarsly BM, Borchardt L, Mechanochemical synthesis of porous carbon at room temperature with a highly ordered sp^2 microstructure, 325–33, Copyright (2018), with permission from Elsevier. D) Reductive dehalogenation approach for the preparation of crosslinked polymers by direct formation of C-C bonds between aromatic rings.³⁵ E) Reactivity of different precursors following the MS study described in Ref.³⁵ Reprinted with permission from Chen H, Fan J, Fu Y, Do-Thanh CL, Suo X, Wang T, Popovs I, Jiang D, Yuan Y, Yang Z, Dai S, Benzene Ring Knitting Achieved by Ambient-Temperature Dehalogenation via Mechanochemical Ullmann-Type Reductive Coupling. *Adv Mater* 2021;33:2008685. Copyright 2021 Wiley. F) Overview of the copolymerisation of lactide with 3S-(isobutyl)morpholine-2,5-dione.³⁶ G) Evolution of molecular weight (dots) and dispersity index (data in blue) for 5, 10 and 15 min reaction time obtained by SEC chromatography compared to theoretical (THEO) values (straight line).³⁶ Reprinted with permission from Burton TF, Pinaud J, Pétry N, Lamaty F, Giani O. Simple and Rapid Mechanochemical Synthesis of Lactide and 3S-(Isobutyl)morpholine-2,5-dione-Based Random Copolymers Using DBU and Thiourea. *ACS Macro Lett* 2021;10:1454–9. Copyright 2021 American Chemical Society.

N-doped HCPs were obtained by direct use of a nitrogen-rich monomer such as 1,3,5-tris(N-carbazolyl)benzene, which was subjected to MS and underwent oxidative polymerisation ($FeCl_3$ as a catalyst and NaCl as a bulking material). The resultant HCPs had an A_{BET} of up to $1710 \text{ m}^2/\text{g}$ after activation ($150 \text{ }^\circ\text{C}$ for 24h under vacuum), which was 100% higher than values previously reported.³⁷ In the same study, S-doped HCPs were also obtained, following the same reaction approach but using 1,3,5-tris(2-thienyl)benzene as monomer. Optimal A_{BET} and yield were obtained after applying a design of experiments approach, which concluded that the $FeCl_3$ /monomer molar ratio is the most influential parameter. Porous materials were only obtained at $FeCl_3$ /monomer molar ratios above 2.5. However, A_{BET} reached a plateau when this ratio was as high as 12. A higher grinding speed of 400 to 800 rpm was instead detrimental to the optimal A_{BET} values, due to the collapse of the structure by applying too much energy. Values of up to $1850 \text{ m}^2/\text{g}$ and $1 \text{ cm}^3/\text{g}$ of A_{BET} and pore volume, respectively, were achieved with a PSD centred in the micropore range with a main peak around 1.6 nm.³⁷

A high level of MS polymerisation was achieved by Ohn et al.¹⁹ by lactide-ring opening, obtaining polylactic acid with a molecular weight as high as $10\,000 \text{ g/mol}$. Both the molecular weight and the yield increased significantly with the grinding time. A much more pronounced trend of increasing molecular weight was observed for the first hour, attributable to the degradation of the high-weight polymer chains by the high energy of MS collisions.

Lactide was also used but in combination with 3S-(isobutyl)morpholine-2,5-dione to produce by MS copolymers with improved biocompatibility and biodegradability (see schematic information in Fig. 3F). First, homo-polymerisations using both precursors were studied, and then with the optimised conditions (reaction time 15 min, molar ratio benzyl alcohol/1,8-diazabicyclo[5.4.0]undec-7-ene (DBU)/3-[3,5-bis(trifluoromethyl)phenyl]-1-cyclohexylthiourea of 1:1:5, DCM 0.2 $\mu\text{L}/\text{mg}$), several copolymers were developed by the modification of the lactide/3S-(isobutyl)morpholine-2,5-dione ratio. The reaction time was studied in the range 5-15 min using the latter precursor, concluding that the molecular weight significantly increased with the reaction time, from about 2 000 g/mol for 5 min to up to 5 000 g/mol for 15 min, see Fig. 3G. The copolymer with the highest molecular weight was the one obtained using a lactide/3S-(isobutyl)morpholine-2,5-dione precursor ratio of 38:12. However, all of them were in a range close to 6 200 – 8 500 g/mol. The glass transition of the polymers was also analysed and they suggested good integration of the monomers.³⁶

Besides, ring opening was used for the polymerisation of different norbornene-based monomers and the co-polymerisation of monomers of different functionality via ruthenium alkylidene initiation. These MS protocols have allowed the production of macropolymers, especially copolymers, which were previously very difficult to obtain, due to the lack of suitable solvents for both monomers, and which made the synthesis protocol tedious and time-consuming. By studying different MS conditions, molecular weights above 20 000 g/mol were obtained by carefully selecting the monomer/initiator ratio and reaction time. Another key feature of the study is that it allowed to see the influence of ball size and quantity on the molecular weight of the polymers developed, concluding that a decrease in ball size also produced a decrease in molecular weight, even when increasing the number of balls. LAG allowed further increases in molecular weights, reaching up to 40 000 g/mol by using tetrahydrofuran (THF) and dichloroethane (DCE) in adequate amounts. By modifying the monomer with different functional groups and dangling chains, macropolymers with molecular weights up to 97 000 g/mol have been reported.³⁸

Grätz et al.³⁹ confirmed that polymerisation took place between a diamine and a dialdehyde (*p*-benzoldicarbaldehyde and *p*-phenylenediamine, respectively) via a MS-induced polycondensation reaction. Different grinding materials and ball sizes were studied, concluding that the higher the energy input, the higher the conversion, which was achieved by using higher density materials and larger ball sizes.

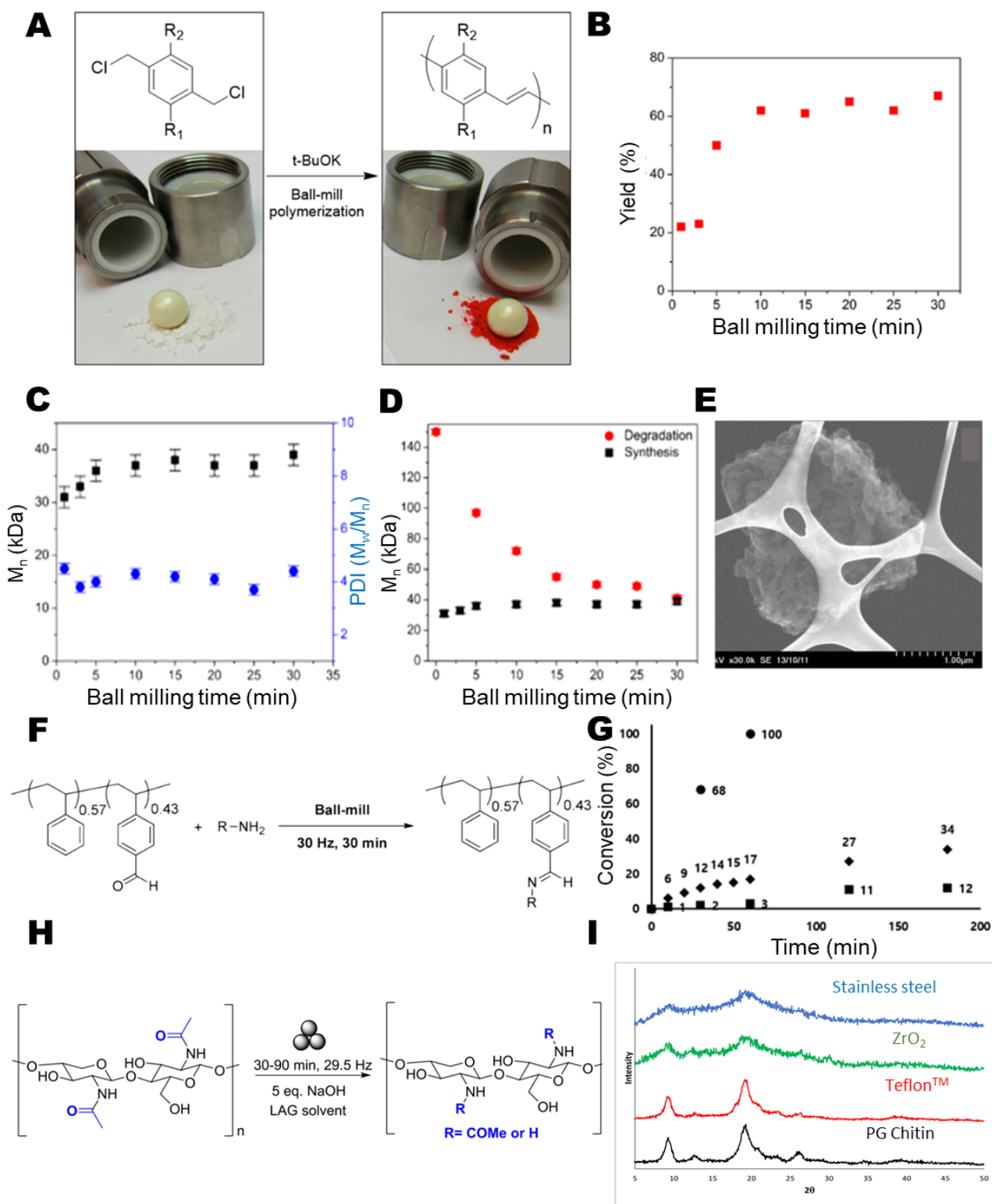


Figure 4. A) Schematic Gilch solid-state polymerisation promoted by ball-milling.⁴⁰ B) Yield as a function of milling time.⁴⁰ C): Number-average molecular weight (M_n) and polydispersity index (PDI) as a function of milling time.⁴⁰ D) M_n as a function of milling time for the synthesis (black squares) of PMEPV-based HCPs prepared in solid-state, and for the degradation (red discs) of PMEPV-based HCPs prepared in solution.⁴⁰ Adapted with permission from Ravnsbæk JB, Swager TM. Mechanochemical Synthesis of Poly(phenylene vinylenes). ACS Macro Lett 2014;3:305–9. Copyright 2014 American Chemical Society. E) SEM image of a TS-based HCP.⁴¹ Reproduced from Ref.⁴¹ with permission from the Royal Society of Chemistry. F) Schematic structure of post-polymerisation modifications by MS in the study of Ohn & Kim.⁴² G) Comparison of conversion between MS and solution reactions (● MS, ■ in $CDCl_3$ at room temperature, ◆ in $CDCl_3$ at 50 °C).⁴² Adapted with permission from Ohn N, Kim JG. Mechanochemical Post-Polymerization Modification: Solvent-Free Solid-State Synthesis of Functional Polymers. ACS Macro Lett 2018;7:561–5. Copyright 2018 American Chemical Society. H) Deacetylation pathway followed by Di Nardo et al.⁴³ I) X-ray diffraction patterns of

chitin and ball-milled chitin using different grinding materials (90 min for TeflonTM, and 30 min for stainless steel and ZrO₂).⁴³ Reproduced from Ref.⁴³ with permission from the Royal Society of Chemistry.

In another study, poly(phenylene vinylene) was produced by MS-based Gilch reactions (schematic representation in Fig. 4A), reaching up a molecular weight of up to 40 000 g/mol and a yield of 70% (see Fig. 4B), where again, the higher the grinding time, the higher the conversion and molecular weight, as shown in Fig. 4C (using poly(2-methoxy-5-2'-ethylhexyloxy phenylene vinylene) (PMEPV) as monomer). However, the scission of different polymeric networks of poly(phenylene vinylene) by MS has also been studied, concluding that polymers with molecular weights above 40 000 g/mol are able to absorb enough energy to cause the scission of their own main chains,⁴⁰ confirming what was observed on A_{BET} or molecular weight reduction in other studies (see Fig. 4D).^{13,15,35,37}

Zhang et al.⁴¹ were also able to prepare polymers (see SEM image in Fig. 4E) with A_{BET} and molecular weight up to 520 m²/g and 485 000 g/mol, respectively, by MS processing of 5,5,6,6-tetrahydroxy-3,3,3,3-tetramethyl-1,1'-spirobisindane and 2,2',3,3'-tetrahydroxy-1,1'-binaphthyl. With reaction times of only 15 minutes, non-highly crosslinked polymers were targeted so that they could be dissolved in common solvents such as THF and DMF. The thermal behaviour showed that no significant changes were observed up to about 400°C, while the residue at 800°C was about 50 wt.%. A low level of highly crosslinked units (around 20%) was also obtained by Pedrazzo et al.⁴⁴ when testing the polymerisation of β-cyclodextrin by MS (4h, 600 rpm). This fraction was evaluated as the water-insoluble fraction. Nevertheless, high molecular weight polymers (up to 22 000 g/mol) were produced. Likewise, poly(ethylene glycol),⁴⁵ poly(*p*-phenylene)³³ and polypyrrole⁴⁶ have been developed by MS procedures.

On the other hand, MS protocols allow not only the polymerisation routes and final products to be modified, but also the polymer itself once it has been obtained. In this sense, Ohn & Kim⁴² tested different polymers using 4-vinylbenzaldehyde as precursor, where successful modifications of the initial polymers were performed (see schematic representation in Fig. 4F). Up to 12 different amines

were tested, ranging from aliphatic to aromatic ones, with conversions of aldehyde substitutions close to 100% in some cases, monitored by ^1H NMR. Compared to solvent-based protocols, at a reaction time of 1h, the conversion increased from 3% at room temperature to 17% at 50 °C, and to 100% for the MS route (see Fig. 4G).

Another interesting future prospect for MS is the production of HCPs derived from bioresources. For example, chitosan can be produced by deacetylation of chitin, which is usually accompanied by a reduction in molecular weight due to some depolymerisation. However, Di Nardo et al.⁴³ reported that MS can produce chitosan with deacetylation levels ranging from 73 to 95%, while maintaining high molecular weights (see a summary of the MS protocol in Fig. 4H). For this purpose, the amorphisation of the initial polymer is a very important step, as crystallinity usually hinders the reactivity of polymers. When testing different grinding materials, those with higher densities (stainless steel and zirconia vs PTFE (TeflonTM)) were able to produce amorphous polymers, as observed by X-ray diffraction (see Fig. 4I), thus confirming their suitability for a better deacetylation protocol.

The main MS parameters and properties of the HCPs obtained from FC and SC are presented in Table 1.

Table 1. Experimental parameters in FC and SC synthesis, and main characteristics of the corresponding HCPs.

Friedel Crafts approach											
Precursor	Ball mill material	Ball mill volume, cm ³	Size, mm (and number) of balls	Reaction time (and pauses), min	Speed (rpm or Hz)	Catalyst (ratio catalyst/monomer)	Crosslinker (ratio crosslinker/monomer)	Yield, %	Surface area, m ² /g	Pore volume, cm ³ /g	Ref.
Benzene	ZrO ₂	45	10 (10)	60 (5)	400	FeCl ₃ (2)	FDA (2)	94	273	0.16	15
Pyrrole	ZrO ₂	45	10 (10)	60 (5)	400	FeCl ₃ (2)	FDA (2)	-	167	0.148	15
Aniline	ZrO ₂	45	10 (10)	60 (5)	400	FeCl ₃ (2)	FDA (2)	64	17	0.014	15
Biphenyl	ZrO ₂	45	10 (10)	60 (5)	400	FeCl ₃ (4)	FDA (4)	-	96	0.123	15
Triphenylbenzene	ZrO ₂	45	10 (10)	60 (5)	400	FeCl ₃ (6)	FDA (6)	-	784	0.34	15
Tetramethylbenzene	ZrO ₂	45	10 (10)	60 (5)	400	FeCl ₃ (10)	FDA (10)	-	23	0.055	15
Benzene	ZrO ₂	45	10 (10)	0.16666667	800	FeCl ₃ (6)	FDA (2)	78	350	-	15
Benzene	ZrO ₂	45	10 (10)	5	800	FeCl ₃ (6)	FDA (2)	99	626	0.588	15
Benzene	ZrO ₂	45	10 (10)	45	800	FeCl ₃ (6)	FDA (2)	95	270	-	15
Benzene	ZrO ₂	45	10 (10)	60	800	FeCl ₃ (6)	FDA (2)	97	260	-	15
Benzene	ZrO ₂	45	10 (10)	120	800	FeCl ₃ (6)	FDA (2)	98	160	-	15
Benzene	ZrO ₂	45	10 (10)	240	800	FeCl ₃ (6)	FDA (2)	99	60	-	15
Stilbene	SS	65	8 (2)	100	-	FeCl ₃ (5.9)	FDA (4.9)	95	375	0.21	30
Tetraphenylethylene	SS	65	8 (2)	100	-	FeCl ₃ (12.3)	FDA (10.2)	115	129	0.14	30
Naphthalene	SS	65	8 (2)	100	-	FeCl ₃ (5.9)	FDA (4.9)	107	71	0.14	30
Toluene	SS	65	8 (2)	100	-	FeCl ₃ (5.6)	FDA (4.6)	98	374	0.25	30
Biphenyl	SS	65	8 (2)	100	-	FeCl ₃ (5.9)	FDA (4.9)	99	556	0.38	30
Scholl Coupling approach											
Pyrrole	ZrO ₂	45	10 (10)	60 (5)	400	FeCl ₃ (2)	-	-	162	0.176	15
Biphenyl	ZrO ₂	45	10 (10)	60 (5)	400	FeCl ₃ (4)	-	83	15	0.029	15
Triphenylbenzene	ZrO ₂	45	10 (10)	60 (5)	400	FeCl ₃ (6)	-	64	82	0.179	15
Tetramethylbenzene	ZrO ₂	45	10 (10)	60 (5)	400	FeCl ₃ (10)	-	67	105	0.161	15
1,3-Bis(N-carbazolyl)benzene	ZrO ₂	20	- (1)	30	30	FeCl ₃ (2.5)	-	83	707	0.45	32
1,3-Bis(N-carbazolyl)benzene	ZrO ₂	20	- (1)	30	30	FeCl ₃ (1.25)	-	52	723	0.45	32
1,3-Bis(N-carbazolyl)benzene	ZrO ₂	20	- (1)	30	30	FeCl ₃ (5)	-	94	678	0.42	32
1,3-Bis(N-carbazolyl)benzene	ZrO ₂	20	- (1)	15	30	FeCl ₃ (2.5)	-	84	394	0.27	32

1,4-Bis(N-carbazolyl)benzene	ZrO ₂	20	- (1)	30	30	FeCl ₃ (2.5)	-	60	780	0.47	32
2,6-Di(9H-carbazol-9-yl)pyridine	ZrO ₂	20	- (1)	30	30	FeCl ₃ (2.5)	-	86	601	0.49	32
3,5-Di(9H-carbazol-9-yl)pyridine	ZrO ₂	20	- (1)	30	30	FeCl ₃ (2.5)	-	83	582	0.46	32
4,4',4"-Tris(carbazol-9-yl)-triphenylamine	ZrO ₂	20	- (1)	30	30	FeCl ₃ (2.5)	-	64	902	0.56	32
1,3,5-Tris(N-carbazolyl)benzene	ZrO ₂	20	- (1)	30	30	FeCl ₃ (2.5)	-	82	935	0.52	32

Crystallinity in HCPs

Although HCPs generally have amorphous structures, porous crystalline structures can also be obtained depending on the choice of precursor and the method of synthesis. These materials, usually referred to as covalent organic frameworks (COFs), have also generally been produced by solvent-based methods,^{47,48} although some examples of MS-based structures can also be found. For instance, in the study of Biswal et al.⁴⁹ three different formulations were prepared by simple mechanical grinding with a mortar and pestle. The latter materials were compared to the same formulations developed by solvothermal methods using 1,3,5-triformylphloroglucinol with: a) an aromatic diamine [*p*-phenylenediamine], b) 2,5-dimethyl-*p*-phenylenediamine, or c) benzidine as HCP precursors. Only 45 min of grinding was sufficient to achieve the same FTIR profile as that observed from solvothermal methods. The samples showed moderate crystallinity and excellent thermal stability up to 350°C, as well as excellent chemical stability in different acidic and basic media, depending on the formulation. However, even after activation at 170°C for 12 h, the samples obtained by mechanical grinding have an A_{BET} of about 60 m²/g at the most, while values between 340 and 540 m²/g were obtained by solvothermal methods. The reason behind these low A_{BET} has been attributed to the layered structure of the mechanically milled samples compared to the

solvothermally obtained samples.⁴⁹ Das et al.⁵⁰ also used *p*-phenylenediamine, terephthalic dihydrazide, 1,3,5-triformylbenzene and 1,3,5-triformylphloroglucinol with a simple mortar by LAG, and compared with solvothermal methods. As Biswal et al. observed, the A_{BET} were much smaller than those obtained by solvothermal methods, which they attributed to the layered structure. Emmerling et al.⁵¹ studied different precursors, such as 2,4,6-tris(4-aminophenyl)-1,3,5-triazine, terephthalaldehyde, benzidine, 1,3,5-triformylbenzene and *p*-phenylenediamine in different combinations for the formation of COFs by MS. Different catalysts and solvents were used, and the increase in crystallinity implied a higher A_{BET} . By using scandium (III) triflate instead of aqueous acetic acid, acting as a catalyst, A_{BET} above 1000 m²/g were obtained and dioxane was better than mesitylene as a solvent.

A positive balance from the perspective of green chemistry principles

In order to understand and better visualise the energy and environmental benefits of MS, an analysis of the 12 principles of green chemistry was carried out,⁵² and is summarised in Fig. 5 in comparison to the traditional solvent-based FC and SC protocols, here referred to as FC_{Sb} and SC_{Sb}, respectively.

The general absence of solvents in MS potentiates the greener approach of the latter and reduces the amount of products involved in the reaction protocol, making MS a better procedure for waste prevention, atom economy, safer solvents and auxiliaries, safer chemistry and safer chemical design. Similarly, the solvents frequently used for FC and SC reactions are hazardous, such as dichloroethane,¹ and require moderate temperatures,¹ making MS a much safer protocol. As mentioned earlier, the reaction time is significantly reduced using MS procedures compared to solvent-based methods, and therefore the energy efficiency is also improved.^{6,15} Nevertheless, there are some principles for which MS of HCPs has not yet provided better performance than FC or SC reaction protocols, such as the lack of bio-based precursors for obtaining high-quality HCPs, or the resultant lack of biodegradability of the obtained products. On the other hand, other principles are well achieved by MS and solvent-based protocols, such as the reduction of derivatives, as the

products obtained are generally homogeneous. The recent development of ball mills that allow both pressure and temperature control has enabled real-time analysis of the reaction.²⁵ The only point where solvent-based protocols outperform MS is the amount of catalyst, as a larger amount is usually required for MS to obtain HCPs of similar surface areas.¹⁵ However, the lack of recoverability of these catalysts, usually metal chlorides, is a general drawback in the synthesis of HCPs. Recent studies have therefore analysed the substitution of these metal chlorides by faster and less harmful species, like trifluoromethanesulfonic acid,⁵³ triflic acid, sulfuric acid or *p*-toluenesulfonic acid.⁵⁴ The latter, which is solid at room temperature, was recovered in yields of over 80% and reused three times without loss of the apparent properties of the products obtained.













Principles of Green Chemistry	MS	FC _{Sb}	SC _{Sb}	Principles of Green Chemistry	MS	FC _{Sb}	SC _{Sb}
 Waste prevention	●	●	●	 Use of renewable feedstocks	●	●	●
 Atom economy	●	●	●	 Reduction of derivatives	●	●	●
 Less hazardous chemical syntheses	●	●	●	 Catalysis	●	●	●
 Designing safer chemicals	●	●	●	 Design for degradation	●	●	●
 Safer solvents and auxiliaries	●	●	●	 Real-time analysis for pollution prevention	●	●	●
 Design for energy efficiency	●	●	●	 Inherently safer chemistry for accident prevention	●	●	●

Figure 5. Analysis of MS, solvent-based FC (FC_{Sb}) and SC (SC_{Sb}) reaction protocols according to the twelve principles of green chemistry. Green, orange and red dots indicate good, average and poor performance against the principle.

A wide range of applications for hyper-crosslinked polymers

HCPs have proven to be valuable in many different application areas due to their inherent porosity. In this section, different applications are discussed in detail, focusing on the latest achievements for each specific case. As mechanosynthesis is a relatively new method for the preparation of HCPs,

their applications in general will be presented here with the aim of encouraging researchers to produce them by more environmentally friendly methods, as is the case for mechanosynthesis.

Catalysis

Extensive work has already been done on the use of HCPs as catalysts, as reported elsewhere.^{3,55} Although there are several studies on metal-free catalysts derived from HCPs^{2,4,55} or based on doping with coordinating atoms such as N, P, O, etc.,^{3,55} the main catalysts have been produced by including metal ligands in the polymer structure.^{3,55,56}

Metal-free HCP-derived catalysts have been used to synthesise biodiesel after esterification of oleic acid and methanol; yields of up to 93% of methyl oleate were obtained under optimal conditions and the reusability of the catalyst was also outstanding, as no significant change in yield was observed after five uses. It should be noted that in the above example, pitch was used as HCP precursor, thus expanding the range of possible precursors to high molecular weight compounds (see the schematic of the HCP synthesis in Fig. 6A). Surface areas of 520 and 380 m²/g were obtained with HCPs functionalised with allyl chloride and those subsequently functionalised with imidazole, respectively, thus producing acidic ionic liquid catalysts immobilized on HCPs acting as supports (see Fig. 6B).² A detailed description of the reaction parameters and catalyst lifetime has been included in Fig. 6C-F. Another reaction that has also been catalysed by HCP-based materials is the conversion of NaN₃ to triazoles and benzylic azides, with conversion efficiencies of up to 95% in EtOH medium.⁵⁷

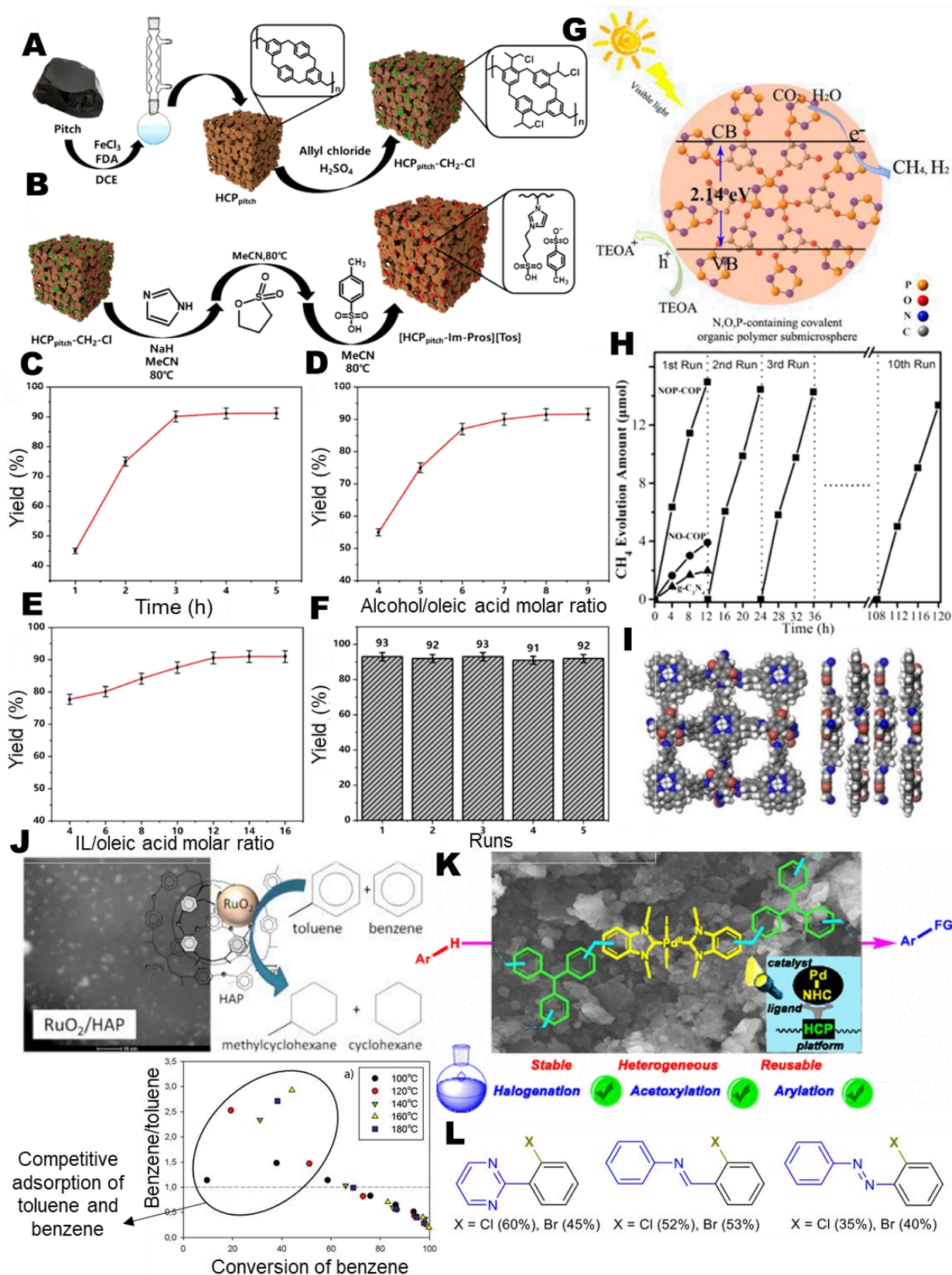


Figure 6. Schematic illustration of the synthesis of: A) pitch-based HCPs functionalised with allyl chloride and B) immobilised acidic ionic liquid catalyst.² Impacts of reaction parameters on the catalysed biodiesel production: C) reaction time, D) alcohol/oleic acid ratio, E) ionic liquid (IL)/oleic acid ratio. F) Yield after several runs of the HCP-based catalyst.² Reprinted with permission from Pei B, Xiang X, Liu T, Li D, Zhao C, Qiu R. Preparation of Chloromethylated Pitch-Based Hyper-Crosslinked Polymers and An Immobilized Acidic Ionic Liquid as A Catalyst for the Synthesis of Biodiesel. *Catalysts* 2019;9:963. Copyright 2019 MDPI. G) Schematic of the photoreduction of CO₂ to CH₄ by P-, O- and N-doped HCPs.⁵⁸ H) CH₄ evolution for several 12h-cycles using the catalysts developed in: NOP-COP (catalyst containing N, O and P), NO-COP (catalyst containing N and O).⁵⁸ Reprinted with

permission from Guo S, Zhang H, Chen Y, Liu Z, Yu B, Zhao Y, et al. Visible-Light-Driven Photoreduction of CO₂ to CH₄ over N,O,P-Containing Covalent Organic Polymer Submicrospheres. *ACS Catal* 2018;8:4576–81. Copyright 2018 American Chemical Society. I) 3D structure of Br-based HCP.⁵⁹ Reprinted with permission from Wang L, Wang R, Zhang X, Mu J, Zhou Z, Su Z. Improved Photoreduction of CO₂ with Water by Tuning the Valence Band of Covalent Organic Frameworks. *ChemSusChem* 2020;13:2973–80. Copyright 2020 Wiley. J) Hydrogenation of a benzene/toluene mixture by a Ru-based HCP, with SEM image and benzene conversion under different conditions.⁶⁰ Reprinted with permission from Bykov AV, Demidenko GN, Nikoshvili LZ, Sulman MG, Kiwi-Minsker L. Hydrogenation of a Benzene-Toluene Mixture Using Metal Nanoparticles Stabilized by a Hyper-Crosslinked Aromatic Polymer. *Chem Eng Technol* 2021;44:1955–61. Copyright 2021 Wiley. K) N,N'-dimethyl-benzimidazolium iodide and triphenylmethane-based HCP catalyst with Pd as the active site.⁶¹ L) Several examples of halogenation reactions promoted by a catalyst developed by Mandal et al.,⁶¹ including yields. Reprinted with permission from Mandal T, Mondal M, Choudhury J. Hypercrosslinked Polymer Platform-Anchored Single-Site Heterogeneous Pd-NHC Catalysts for Diverse C-H Functionalization. *Organometallics* 2021;40:2443–9. Copyright 2021 American Chemical Society.

As with the inclusion of N, P and O, the combination of barbituric acid and hexachlorocyclophosphazene allowed the preparation of efficient catalysts for the photoreduction of CO₂, capable of producing up to 22.5 μmol/(g·h) CH₄ with a 90% selectivity (see the schematic of the catalytic activity in Fig. 6G).⁵⁸ This optimal catalyst showed very good performance even after more than 10 cycles of 12 h duration, as observed in Fig. 6H. Other atoms such as Br were also used to develop organic frameworks in which the delocalisation caused by this atom could help to reduce CO₂ to CO with a selectivity of almost 96% and a yield of about 300 μmol/g for 12 h (see 3D molecular representation in Fig. 6I).⁵⁹ By combining imidazole and octavinylsesquioxane, HCPs with surface areas up to 537 m²/g and having micro- and mesoporosity were obtained, which again acted as efficient catalysts for CO₂ conversion.⁶² S-functionalised HCPs were formulated by Li et al.,⁶³ showing very good results for the rearrangement of cyclohexanone oxime. More examples based on N- and S-doped HCPs can be found in the study of Gu et al.³

Regarding HCP-based catalysts that include metal compounds in their structure, HCPs have been applied as supports for NiOOH and SiO₂, used as the active phase and Brønsted acid, respectively, demonstrating the ability to produce hydrocracking of anthracene in supercritical propanol.⁶⁴ The hydrogenation of benzene in benzene/toluene mixtures can also be catalysed by amino-HCP-based catalysts, where the active sites were provided by three different metals: Pt, Pd and Ru. A selectivity of 44% towards cyclohexane and an almost complete conversion of benzene were achieved under optimal conditions using Ru as the active metal ligand (see overview in Fig. 6J).⁶⁰ In another study, Pd-derived HCPs (see Fig. 6K) catalysed C–H halogenation, acetoxylation, and arylation with yields

up to 85, 75 and 70%, respectively (see some examples of halogenation reactions in Fig. 6L) These HCPs were based on *N,N'*-dimethyl-benzimidazolium iodide and triphenylmethane.⁶¹ Suzuki-Miyaura reactions were also catalysed by Pd-based HCPs with a very low Pd content of only 0.03 mol.% achieving up to 6 complete cycles without significant loss of activity.⁶⁵ Other reactions have also been subjected to the use of Pd-based catalysts associated with HCPs.^{66,67} In the case of the catalytic conversion of CO₂, Du et al.⁵⁵ summarised the state-of-the-art of HCP-based metal ligands catalysts. Other examples of HCPs doped with metal complexes and/or nanoparticles with application in catalysis were reported by Gu et al.³ and Valverde-González et al.,⁵⁶ concluding that palladium and ruthenium are the most used metals for catalyst formulations, while triphenylphosphine is the most used precursor for HCP formation. While no relationship could be found between surface area and catalytic activity, a higher activity was found to be correlated with smaller nanoparticles.

Chromatography

Due to the possibility of tailoring their porosity, HCPs have also been used in chromatography. For example, Shirayeva et al.⁶⁸ developed a polystyrene-based HCP that was used as a stationary phase in gas chromatography. Although it mimicked the structure of the widely used poly(trimethylsilylpropyne) quite well, a limited porous network was obtained, which could not perform as well as the aforementioned phase for light hydrocarbons. However, more recent studies by Kanateva et al.⁶⁹ succeeded in preparing suitable and highly efficient HCPs for gas chromatography column (see Fig. 7A), using the same precursor as in the previous study, and which achieved high resolution for the separation of volatile compounds, such as ethane, ethene and ethyne, and many others depending on the selected conditions, as can be seen in Fig. 7B and C. In addition, this HCP exhibited high water resistance and thermal stability.

With regard to liquid chromatography, Penner et al.⁷⁰ have already studied the use of hyper-crosslinked polystyrene as a substitute for common column materials of in 1999. These HCPs were

able to successfully separate many aromatic compounds, such as 2,4-dinitrophenol, phenol, *p*-nitrophenol, *o*-nitrophenol, dimethyl phthalate, diethyl phthalate and di-*n*-propyl phthalate, among others. Tsyurupa et al.⁷¹ also used styrene-based HCPs, but based on divinylbenzene as a copolymer, to completely separate acetone, benzene, naphthalene, anthracene, toluene, *p*-nitrophenol and 2,6-dinitrophenol. Using instead cholesteryl methacrylate together with other aromatic compounds, HCPs were successfully tested as capillary columns for the separation of alkylbenzenes, *o*-terphenyl/triphenylene, parabens, and proteins. The overall separation efficiency was excellent and comparable to other commercial columns.⁷²

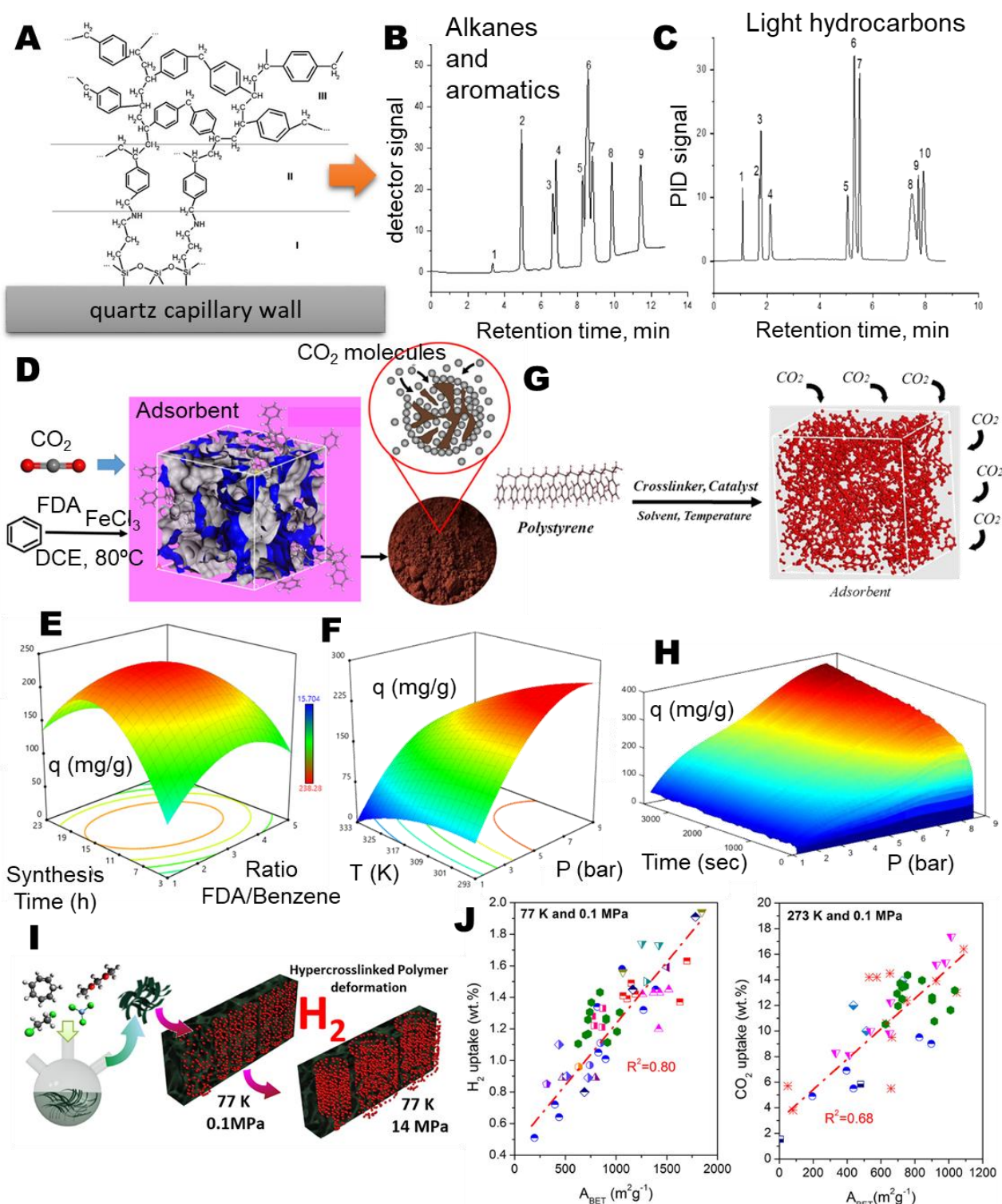


Figure 7. Capillary column with a bonded layer of hyper-crosslinked polystyrene.⁶⁹ B) Separation of n-alkanes C6–C10 and aromatic compounds on the HCP-derived column. Solutes: 1, n-pentane; 2, n-hexane + benzene; 3, n-heptane; 4, toluene; 5, n-octane; 6, ethylbenzene + *m*-xylene + *p*-xylene; 7, *o*-xylene; 8, n-nonane; 9, n-decane. C) Separation of light hydrocarbons on the HCP-derived column. Solutes: 1, methane; 2, ethylene; 3, acetylene; 4, ethane; 5, propene; 6, propane + allene; 7, propine; 8, isobutene; 9, butadiene; 10, n-butane.⁶⁰ Reprinted with permission from Kanateva AY, Korolev AA, Kurganov AA. Preparation and properties of GC capillary column with hypercrosslinked stationary phase. *J Sep Sci* 2021;44:4395–401. Copyright 2021 Wiley. D) Schematic representation of the synthesis and CO₂ adsorption of a benzene-based HCP, with E) the effect of FDA/benzene ratio and synthesis time on the adsorption capacity at a pressure of 7 bar and a temperature of 35 °C, and F) the effect of pressure and temperature on the adsorption capacity for an FDA/benzene ratio of 3 and synthesis time of 13 h.⁷ Adapted with permission from Ramezanipour Penchah H, Ghaemi A, Ganadzadeh Gilani H. Benzene-Based Hyper-Cross-Linked Polymer with Enhanced Adsorption Capacity for CO₂ Capture. *Energy and Fuels* 2019;33:12578–86. Copyright 2019 American Chemical Society. G) Schematic representation of a polystyrene-based HCP adsorbent, with H) CO₂ adsorption capacity as a function of pressure and time for the optimum conditions and I) Hypercrosslinked Polymer deformation under H₂ at 77 K and 0.1 MPa and 14 MPa. J) H₂ uptake (wt.%) and CO₂ uptake (wt.%) versus BET surface area (m²g⁻¹) at 77 K and 0.1 MPa, and 273 K and 0.1 MPa, with R² values of 0.80 and 0.68 respectively.

a temperature of 25 °C.⁷³ Reprinted by permission from Springer Nature Customer Service Centre GmbH: Springer, Polymer Bulletin, Efficiency increase in hyper-crosslinked polymer based on polystyrene in CO₂ adsorption process, Ramezanipour Penchah H, Ghaemi A, Ghanadzadeh Gilani H. Copyright 2020. I) Summary of HCP formation using benzene as precursor by FC reaction and its performance on hydrogen storage at different pressures.⁶ J) Review of H₂ and CO₂ uptakes of HCPs by Ramirez-Vidal et al.⁶ Reprinted from Journal of Colloid and Interface Science, 605, Ramirez-Vidal P, Suárez-García F, Canevesi RLS, Castro-Muñiz A, Gadonneix P, Paredes JI, Celzard A, Fierro V, Irreversible deformation of hyper-crosslinked polymers after hydrogen adsorption, 513–27, Copyright (2022), with permission from Elsevier.

Adsorption

Gaseous compounds

The usually high porosity of HCPs has placed them among the most promising materials for the adsorption of many different gaseous compounds. This, together with the growing concern about CO₂ emissions, is leading many researchers to focus their efforts on this topic.^{8,9,74–76} CO₂ adsorption has been performed on benzene-based HCPs, achieving maximum storage values of 262 mg/g (see schematic summary in Fig. 7D, and main performance based on different parameters in Fig. 7E and 7F).⁷ HCPs based on polystyrene (100 000 g/mol) were also studied for CO₂ adsorption using a surface response methodology, from which values of surface area up to 370 m²/g were obtained. Optimal CO₂ adsorption (222 mg/g at 5 bar) was achieved at 14.6 h reaction time, with 0.01 mmol polystyrene, 15 mmol FeCl₃ and 17.7 mmol FDA (the schematic representation is given Fig. 7G, also including the effect of pressure and time on the adsorption capacity, Fig. 7H).⁷³ Other examples of HCP based on polystyrene have been summarised by Castaldo et al.⁵

H₂ storage is also receiving a lot of attention due to the need to replace fossil fuels and to provide alternative means of energy. Ramirez-Vidal et al.⁶ evaluated H₂ storage up to high pressures of 14 MPa. HCPs showed irreversible deformation at these high pressures, which limits their field of application (see summary in Fig. 7I). A detailed review of H₂ and CO₂ adsorption data reported in the open literature was also carried out: Fig. 7J shows H₂ adsorption at -196 °C and 1 atm, and CO₂ adsorption at 0 °C and 1 atm, as a function of the BET area of HCPs.⁶

Methane adsorption was also studied with HCP frameworks. Thus, using tetraphenylmethane and FDA as precursor and crosslinker, respectively, A_{BET} values in the range of 950-1300 m²/g were

obtained depending on the precursor/crosslinker ratio. When the sample with the highest A_{BET} was tested for methane adsorption at 10 bar, capacities as high as 84 and 64 cm^3/g at 0 and 25°C, respectively, were obtained.⁷⁷ The porous carbons developed from these HCPs also exhibited very good CH_4 adsorption capacities.⁷⁸ In another study by Wood et al.,⁷⁹ HCPs were prepared from dichloroethylene and 4,4'-bis(chloromethyl)-1,1'-biphenyl and, depending on the precursor, different values of A_{BET} and CH_4 uptakes were obtained, with a maximum of 5.2 mmol/g at 20 bar for the sample with the highest A_{BET} , 1904 m^2/g . These results are significantly higher adsorption than those obtained by Errahali et al.,⁷⁷ 3.75 and 2.86 mmol/g at 0 and 25°C, respectively. Even higher CH_4 uptakes were reported by Tong et al.⁸⁰ when preparing polystyrene-based HCPs, which reached 9.75 mmol/g at 65 bar and 0 °C for materials having an A_{BET} of about 2085 m^2/g .

Organic vapours can also be adsorbed by HCPs, as demonstrated by Grätz et al.,¹³ where 4,4'-bis(chloromethyl)-1,1'-biphenyl-based HCPs gave excellent results for the adsorption of benzene and cyclohexane. In another study, trichloroethylene was successfully adsorbed by poly(styrene-divinylbenzene)-based HCPs. Different parameters, such as flow rate, column height/diameter ratio and temperature were analysed; it was concluded that an increase in temperature and flow rate led to a reduction in adsorption capacity, while an increase in height/diameter ratio from 1 to 2 led to a significant improvement and then retention of adsorption capacity up to a height/diameter ratio of 5.⁸¹ Data on the adsorption of other volatile organic compounds by HCPs, including a comprehensive analysis of key parameters, have been reported by Li et al.⁸²

Liquid-phase compounds

Removal of organic molecules

The adsorption of organic compounds, including dyes, in the liquid phase was studied using HCPs. As an example, uptakes of naphthalene and 1-naphthylamine of 226 and 175 mg/g were respectively obtained by adsorption in an HCP based on poly(*p*-(2,2,2-triphenylethyl)styrene). This system was

able to maintain adsorption capacities of about 72% and 89% of the initial uptake after five cycles.¹⁰ Various phenolic compounds such as salicylic acid, phenol, hydroquinol, phlorogucinol and gallic acid were also tested for adsorption by a series of HCPs with a chloromethylated polystyrene backbone, with and without functionalisation with amino, hydroxyl, and other complex functional groups. The inclusion of isatin in the polymer network allowed the adsorption of up to 336 mg/g of salicylic acid, more than twice the capacity of the non-functionalised HCP, and between 3 and 6 times the capacity of commercial resins.¹²

In another study, hyper-crosslinked cyclodextrin-based membranes with graphitic acid as a "green" precursor were fabricated (see Fig. 8A for a schematic overview), which were tested for the adsorption of pyrene, phenanthrene, fluoranthene and benzopirene. The highest adsorbed amounts were 25, 14, 17.5 and 24 mg/g, respectively.⁸³ Besides, the adsorption of common dyes such as safranin O (SO), methylene blue chloride (MB) and rhodamine B (RhoB) was evaluated, reaching a plateau around 1000 min, with uptakes close to 200 mg/g, as can be seen in Fig. 8B. In this sense, Castaldo et al.⁷⁴ developed an amino-functionalised HCP based on vinylbenzyl chloride/divinylbenzene, which was able to adsorb up to 130 mg/g of indigo carmine, more than four times the amount adsorbed by non-functionalised HCPs. Focusing on the removal of methyl orange, imidazolium- and pyridine-based HCPs were able to achieve adsorption capacities as high as 1159 mg/g, significantly exceeding the values obtained by previous studies with more common sorbents.⁸⁴ Using two different precursors, namely tetraphenylethylene and 4-(5,6-diphenyl-1H-benzimidazol-2-yl)-triphenylamine, crosslinked with 1,4-bis(chloromethyl)benzene, rhodamine B adsorbed amounts of up to 107 and 256 mg/g were obtained by HCPs based on the former and latter precursor, respectively.⁸⁵ Guerritore et al.⁸⁶ evaluated another way to increase the adsorption capacity by including silica nanoparticles in a styrene-based HCP backbone, which resulted in Remazol Brilliant Blue R adsorption uptakes above 200 mg/g. More comprehensive information on this topic has been reported elsewhere.^{11,87}

However, before implementing any of these systems (or a combination of them) in real wastewater treatment plants, further studies have to be developed regarding the actual removal in complex wastewater, where many different dyes (as done by Anito et al.⁸⁸ for metal ion removal) and other compounds are present. In this sense, not only the removal of dyes should be studied, but also the selectivity and inhibition caused by other compounds coexisting in the wastewater, which is vital for the actual performance of adsorbents. Other examples with more toxic dyes, like Congo red, eriochrome black T, crystal violet, etc. have been extensively evaluated by Waheed et al.¹¹

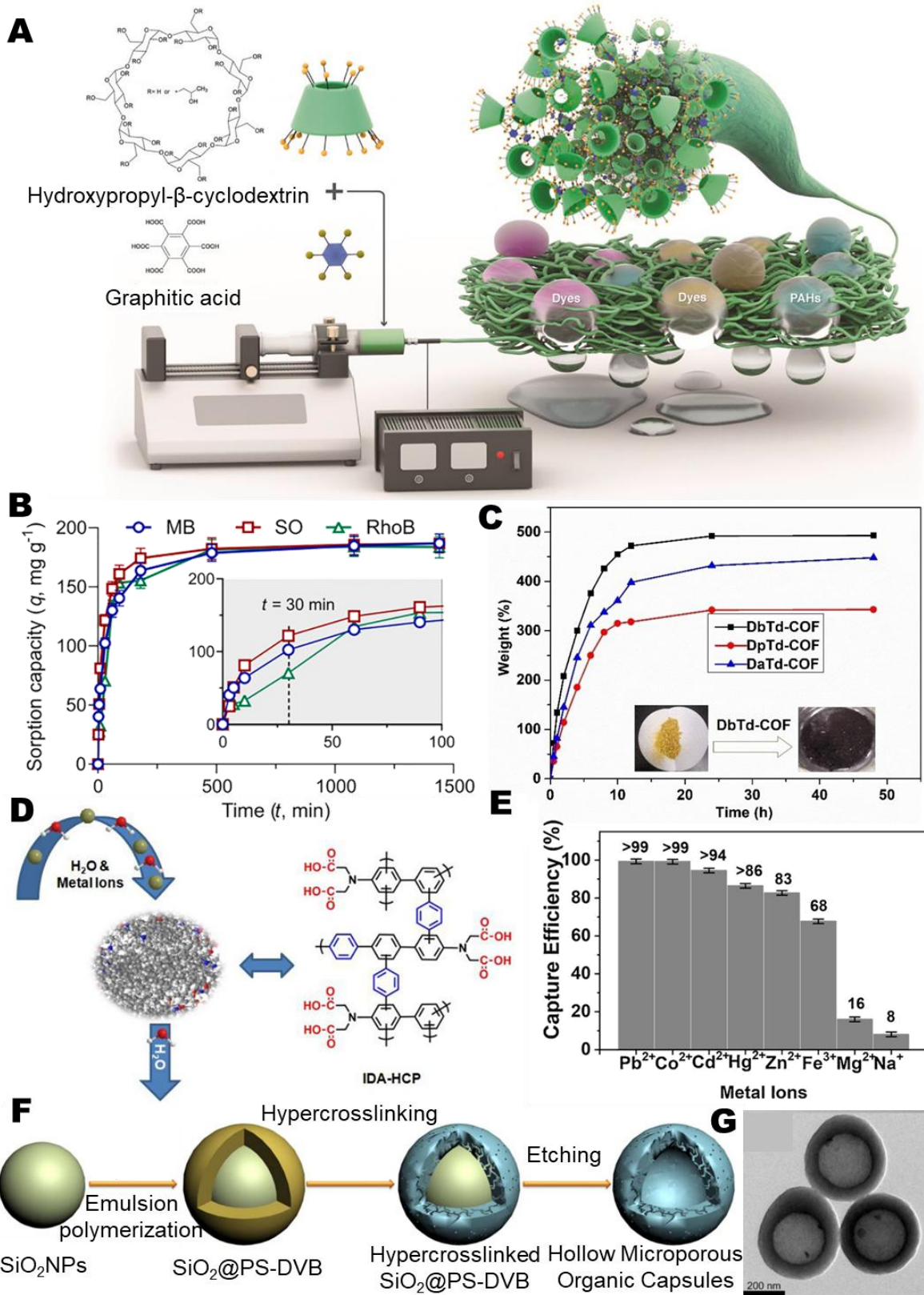


Figure 8. A) Schematic fabrication of hyper-crosslinked cyclodextrin networks using a graphitic acid crosslinker with the scavenging of organic micropollutants from water, and B) sorption capacity as a function of time for several dyes (SO, Safranin O; MB, methylene blue chloride; RhoB, rhodamine B).⁸³ Reprinted from Chemical Engineering Journal, 419, Topuz F, Holtz T, Szekely G, Scavenging organic micropollutants from water with nanofibrous hyper-crosslinked cyclodextrin membranes derived from green resources, 129443, Copyright (2021), with permission from Elsevier. C) Iodine adsorption curves of different HCPs at 75 °C (inset: colour of a HCP before and after iodine capture).⁸⁹ Reprinted with permission from Wu Z, Wei W, Ma J, Luo J, Zhou Y, Zhou Z, Liu S. Adsorption of Iodine on Adamantane-Based Covalent Organic Frameworks. ChemistrySelect 2021;6:10141–8. Copyright 2021 Wiley.

D) Schematic illustration of iminodiacetic acid-functionalised HCPs and their E) capture efficiency for the removal of various metallic ions.⁸⁸ Reprinted from Journal of Hazardous Materials, 400, Anito DA, Wang TX, Liu ZW, Ding X, Han BH, Iminodiacetic acid-functionalized porous polymer for removal of toxic metal ions from water, 123188, Copyright (2020), with permission from Elsevier. F) Schematic formation route of hollow HCP-based microspheres, and G) corresponding SEM images.⁹⁰ Reprinted by permission from Springer Nature Customer Service Centre GmbH: Springer, Scientific Reports, Hollow Microporous Organic Capsules, Li B, Yang X, Xia L, Majeed MI, Tan B, Copyright 2013.

Removal of inorganics

The removal of inorganic matter, including heavy metals, is also a frequently discussed topic, as these chemicals endanger human health and the environment. For example, iodine removal has been studied, with up to 2600 mg/g uptake for a trypticene-based HCP,⁷⁶ while adsorbed amounts up to 4900 mg/g were obtained considering 1,3,5,7-tetrakis (4-formylphenyl) adamantane as a precursor, as shown by the iodine adsorption curves in Fig. 8C.⁸⁹

Based on a carbazole backbone, HCPs with surface area and pore volume of 689 m²/g and 0.54 cm³/g, respectively, were able to remove up to 99.88% of Pb²⁺ ions from wastewater under optimal conditions (*i.e.*, 35 °C, 40 mg/L Pb²⁺, pH 11 and adsorption time of 60 min).⁹¹ In a more comprehensive study, iminodiacetic acid-functionalised HCPs (see schematics in Fig. 8D) were used to study the selectivity in the removal of various metal ions simultaneously, which is close to a real-life scenario. The HCPs significantly removed Hg²⁺, Co²⁺, Pb²⁺ and Cd²⁺ species (see Fig. 8E) in a solution containing Fe³⁺, Cd²⁺, Pb²⁺, Mg²⁺, Hg²⁺, Co²⁺, Zn²⁺ and Na⁺.⁸⁸ Using poly(*para*-methoxystyrene) as a precursor, Fe³⁺ ions in aqueous solution were also removed.⁹² The removal of other toxic metal ions by HCPs has also been discussed in studies by Waheed et al.¹¹ and Masoumi et al.,¹⁴ demonstrating that HCPs can be applied in a wide range of settings, depending on the precursor, the metal species involved and different scenarios.

Drug delivery

The highly porous structure of HCPs can allow drugs to be appropriately confined within the polymeric backbone, making them promising carriers for drug delivery. In this sense, HCP-based hollow microspheres containing silica nanoparticles were developed by Li et al.,⁹⁰ using both polystyrene and divinylbenzene as precursors, which were able to tune the adsorption and thus the

drug delivery capacity by carefully choosing the concentration of the silica nanoparticles (see the schematic preparation process of these hollow microspheres in Fig. 8F and the actual SEM image in Fig. 8G). Thus, the release of ibuprofen in simulated body fluid (37 °C, pH 7.4) was evaluated, showing that at low concentrations of silica nanoparticles (0.5-5%), ibuprofen can be released almost completely within a period of 25 hours, whereas it is much faster (around 12 hours) for higher concentrations (10-15%), due to the presence of much smaller pores. In addition, the release response also shifts from first-order to zero-order kinetics when the silica concentration increases to 10-15%. In a different approach, HER2, a receptor well known to recognise a wide variety of cancer cells, was hyper-crosslinked with N-(2-hydroxypropyl)methacrylamide to enhance its internalisation into the cells, allowing its delivery beyond the cell wall, and enabling detection of the tumour at earlier stages.⁹³ On the other hand, cyclodextrin, this time part of a co-HCP with sialic acid, proved valuable for the adsorption and encapsulation of organic compounds, and the site-specific targeting properties of sialic acid were exploited simultaneously. Doxorubicin was chosen as a model to test the release of the drug, which showed strong adsorption on the thus synthesised HCPs, and allowed adequate discharge into the cells, assessed by confocal microscopy. In addition, it is worth mentioning that no cytotoxic effect was found.⁹⁴ More detailed information on HCPs with applications in drug delivery, with particular attention to nanosponges and cyclodextrin-based systems, is available elsewhere.⁹⁵⁻⁹⁹

Bio-based HCPs

The use of bioresources for the production of high value-added HCPs has not been studied in depth to date, which we consider to be a gap in this research area. In this section, studies that take advantage of bioresources to formulate HCPs are reviewed.

Lignin, a well-known by-product of paper and bioethanol production, was used for the formulation of HCPs with FDA by Meng and Weber (see schematics and SEM image of the HCP in Fig. 9A).¹⁰⁰

Although no suitable porous structure was produced by the solvent-based FC reaction, since surface areas around 5 m²/g were obtained, an acceptable CO₂ adsorption capacity with outstanding selectivity against N₂ was reported (see Fig. 9B (left)). The carbonaceous materials obtained after heat treatment at 550 °C adsorbed larger amounts of CO₂ and N₂, but the selectivity in CO₂ separation was reduced (see Fig. 9B (right)). Lignin-based HCPs were synthesised by Liu et al.,¹⁰¹ but this time by copolymerization with 4-vinylbenzyl chloride and divinylbenzene. Contrary to what was observed by Meng and Weber,¹⁰⁰ the inclusion of such copolymers increased the A_{BET} to values between 1000 and 1450 m²/g. These HCPs showed very good iodine uptake, with maximum capacities of around 250 wt.% at 75 °C and 1 bar, comparable to those observed for the trypticene-based HCP reported in a previous section.¹⁰² In a different approach, smaller units derived from lignin, such as guaiacol, *p*-methoxyphenol, *m*-methoxyphenol, 4-ethylphenol and others, have also been used as precursors for HCP formation.¹⁰³ Again, although the A_{BET} were less than 250 m²/g, CO₂ and iodine uptake were found to be as high as 64.1 mg/g (at 0 °C and 1 bar) and 192.3 wt.%, respectively, were reported. The latter results are very close to the CO₂ uptake obtained by using lignin-derived HCPs in the work of Meng and Weber (61.5 mg/g at 0 °C and 1 bar). A selectivity of 35 was obtained when studying a CO₂/N₂ mixture, somewhat lower than that of the HCP derived from Organosolv lignin (see Fig. 9B (left)). In an even greener approach, cashew nut shell liquid was used as a precursor of several HCPs by SC reaction in DCE. A_{BET} of less than 95 m²/g were obtained but very good *o*-xylene adsorption performance, up to 217 mg/g, was achieved and only slightly reduced (by 7%) after five adsorption/desorption cycles.¹⁰⁴

On the other hand, catechol, a dihydroxybenzene, has been recently used as bio-precursor of HCP using FDA as a crosslinker by a solvent-based FC reaction. This HCP was successfully used to remove Fe²⁺ from water. Indeed, catechol possesses high inherent affinity for Fe ions, due to the positions of their functional groups, which was confirmed by the selection of other monomers, such as toluene, phenol and hydroquinone. Thus, the HCP derived from catechol presented the highest

Fe²⁺ uptake, reaching more than 80 wt.% adsorption of the Fe²⁺ concentration in solution, compared to about 20 wt.% for the HCPs derived from the other monomers (see Fig. 9C), even though the A_{BET} was much higher for the toluene-based HCP (745 m²/g) compared to the others (ranging from 3 to 32m²/g).¹⁰⁵ HCPs synthesised from catechol, FDA and using a solvent-based FC reaction were also used as supports for silver nanoparticles, and the materials showed high antibacterial activity. Damage to the cell structure was observed by examining SEM images of cultures with and without the presence of Ag in the HCPs (see Fig. 9D).¹⁰⁶

β-myrcene, a terpene that can be recovered from essential oils, was used with 4-vinylbenzyl chloride, divinylbenzene and 1,3-butanedioldiacrylate, used as crosslinkers, to produce HCPs.¹⁰⁷ The maximum A_{BET} was 60 m²/g and these materials were considered as potential porous hosts for phase-change materials.

The partial substitution of non-renewable feedstocks was studied by Zhou et al.¹⁰⁸ In their work, cassava starch functionalised with styrene was used as a precursor for the formulation of HCPs using different crosslinkers, namely FDA, 1,4-dichlorobenzene and 4,4'-bis(chloromethyl)-1,1'-biphenyl. It was found that the larger the size of the crosslinker used, the higher the A_{BET} of the HCPs, increasing from 222 m²/g for FDA to 791 m²/g for 1,4-dichlorobenzene and 818 m²/g for 4,4'-bis(chloromethyl)-1,1'-biphenyl. The latter HCP showed good uptake of organic compounds, reaching 2.82 mmol/g of acetophenone (see Fig. 9E), and with an acetophenone/1-phenylethanol selectivity close to 5:1. Furthermore, the efficiency using wastewater with traces of other toxic compounds such as phenol, toluene, benzyl alcohol, etc., and with a higher concentration of 1-phenylethanol compared to acetophenone was also demonstrated (93.6% and 74.4% removal of acetophenone and 1-phenylethanol, respectively), as shown in Fig. 9F. In a similar approach, starch- and styrene-based HCPs were synthesised by varying the concentration and molar ratios of FeCl₃ and FDA. The optimal formulation, with FeCl₃/FDA and FDA/styrene molar ratios of 2.5:1 and 10:6 respectively, resulted in maximum A_{BET} values of 1039 m²/g, with a total pore volume of 0.71 cm³/g,

which allowed for the maximum adsorption of bisphenols (bisphenol A (BPA), bisphenol AF (BPAF), bisphenol F (BPF) and bisphenol S (BPS)) (see Fig. 9G).¹⁰⁹

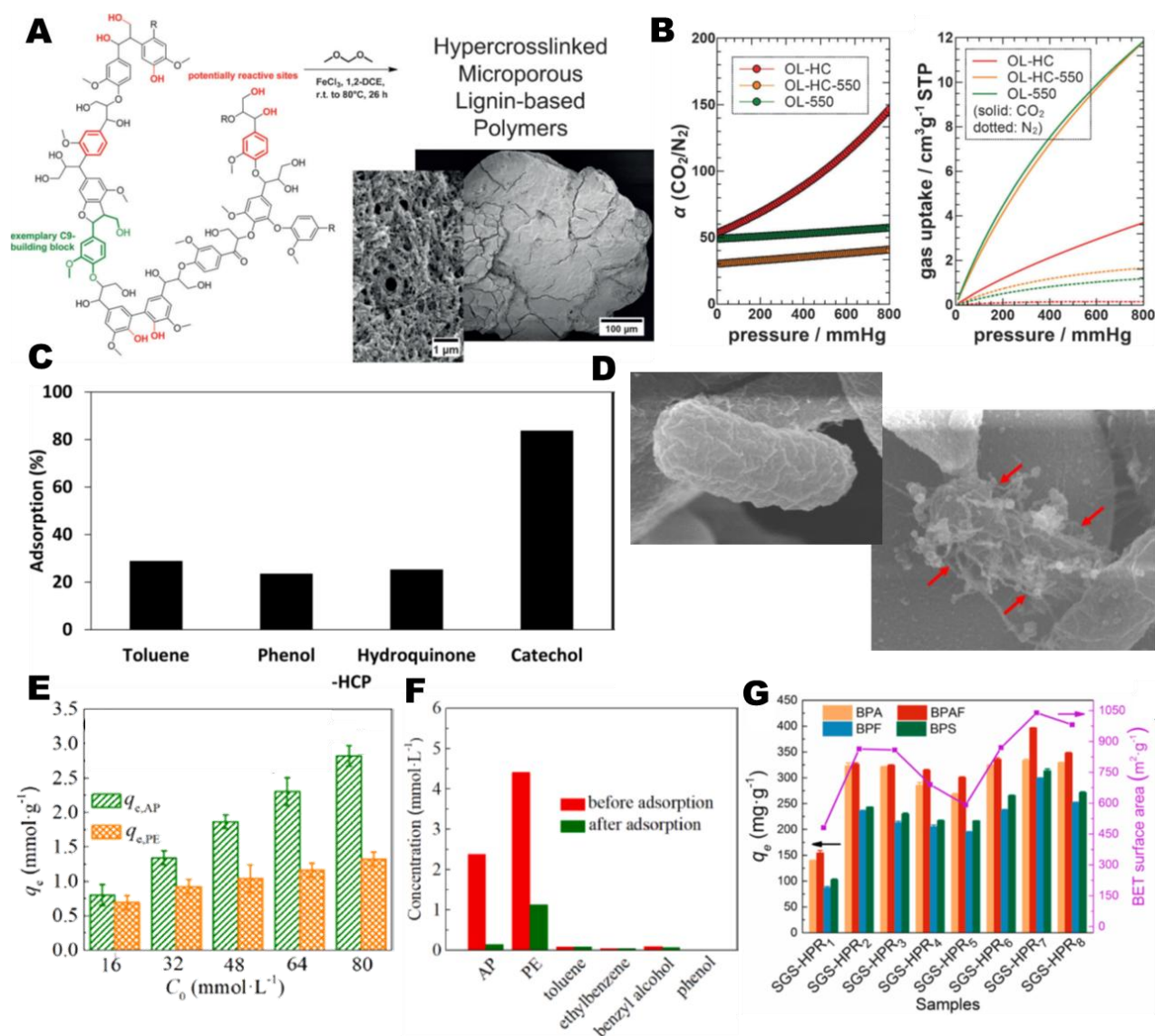


Figure 9. A) Schematic overview of lignin-based HCP formulation, including SEM images of the resulting HCPs.¹⁰⁰ B) (left) CO₂/N₂ selectivity and (right) gas uptake for the lignin-based HCP (OL-HC) and high-temperature-treated HCP (OL-HC-550) and lignin (OL-550).¹⁰⁰ Reprinted with permission from Meng QB, Weber J. Lignin-based microporous materials as selective adsorbents for carbon dioxide separation. *ChemSusChem* 2014;7:3312–8. Copyright 2014 Wiley. C) Adsorption of Fe²⁺ in solution for different aromatics-based HCPs [85]. Reprinted by permission from Springer Nature Customer Service Centre GmbH: Springer, *Journal of Polymers and the Environment*, Bio- inspired Catechol- based Hyper-crosslinked Polymer for Iron (Fe) Removal from Water, Ratvijitvech T. Copyright 2020. D) SEM images of *Escherichia coli*, before (left) and after (right) addition of Ag nanoparticles to HCPs. Red arrows indicate cell damage.¹⁰⁶ Reprinted from *Materials Today Communications*, 28, Ratvijitvech T, Pombejra SN, Antibacterial efficiency of microporous hyper-crosslinked polymer conjugated with biosynthesized silver nanoparticles from *Aspergillus nige*, 102617, Copyright (2021), with permission from Elsevier. E) Adsorption of acetophenone (AP) and 1-phenylethanol (PE) as a function of initial concentrations for 4,4'-bis(chloromethyl)-1,1'-biphenyl-based HCP at 25 °C.¹⁰⁸ F) Adsorption results obtained in real wastewater by the action of an HCP based on 4,4'-bis(chloromethyl)-1,1'-biphenyl.¹⁰⁸ Reprinted from *Chemical Engineering Journal*, 418, Zhou L, Chai K, Yao X, Ji H, Enhanced recovery of acetophenone and 1-phenylethanol from petrochemical effluent by highly porous starch-based hyper-crosslinked polymers, 129351, Copyright (2022), with permission from Elsevier. G) Adsorption of different bisphenols, along with surface area, of different starch- and styrene-based HCPs.¹⁰⁹ Reprinted from *Chemical Engineering Journal*, 429, Yuan W, Zhou L, Zhang Z, Ying Y, Fan W, Chai K, Zhao Z, Tan Z, Shen F, Ji H, Synergistic dual-functionalities of starch-grafted-styrene hydrophilic porous resin for efficiently removing bisphenols from wastewater, 132350, Copyright (2022), with permission from Elsevier.

Although some studies to produce bio-based HCPs have been carried out, there is still a lot of work to be done, as very low surface areas are usually obtained, which limits the application of these materials. Therefore, in this review, we have provided in-depth knowledge on different topics, in order to combine the use of a simple, fast and green technology such as MS, with the need to use bio-based precursors instead of molecules derived from petrochemistry. We have highlighted the potential applications of these materials, so that the scientific community can have a basis for further improvements in this field.

Conclusion

The present review gathers, among other greener synthesis methods, the latest achievements in mechanosynthesis (MS) of hyper-crosslinked polymers (HCPs) based on different approaches, mainly Friedel-Crafts (FC) and Scholl coupling (SC) reactions, but also other less common procedures. We have analysed in detail the different experimental parameters in each considered approach and have paid special attention to the porosity obtained. Depending on the precursor, the presence/absence of crosslinker, and the nature of the crosslinker used and the MS parameters (jar and ball materials, rotation speed, reaction time, etc.), a wide range of different HCPs can be formulated, with pore textures ranging from very low BET area values to more than 1000 m²/g.

The greenest and most efficient approach was MS compared to solvent-based reactions, such as FC and SC, and this was concluded after analysing the twelve principles of green chemistry for the three synthesis methods. A section including the main applications of HCPs was also presented, with special attention paid to the fields of catalysis, chromatography, adsorption and drug delivery, where these HCPs have shown outstanding performance. Finally, a last section concerning the use of bioresources in HCP formulations was included, which would further enhance the greener aspects of the MS approach. Therefore, this review is not only a summary of the different approaches considered for the synthesis of HCPs, but also a call to the scientific community to produce them in a greener, faster and simpler way through the use of bioresources and MS.

Author contributions

A.M. Borrero-López: Investigation, Conceptualization, Writing – original draft, Writing – review & editing;

A. Celzard: Supervision, Validation, Writing – review & editing; V. Fierro: Funding acquisition, Project administration, Conceptualization, Supervision, Validation, Writing – review & editing.

Acknowledgments

This work was partially funded by the European Union (EU) Research Fund for Coal and Steel (RFCS) under Grant Agreement No 101033964 and by the European Regional Development Fund (ERDF) projects TALiSMAN and TALiSMAN 2. A.M.B.-L. also thanks the Margarita Salas grant (SOL-RPU-59) received.

References

- [1] Huang J, Turner SR. Hypercrosslinked Polymers: A Review. *Polym Rev* 2018;58:1–41. <https://doi.org/10.1080/15583724.2017.1344703>.
- [2] Pei B, Xiang X, Liu T, Li D, Zhao C, Qiu R. Preparation of Chloromethylated Pitch-Based Hyper-Crosslinked Polymers and An Immobilized Acidic Ionic Liquid as A Catalyst for the Synthesis of Biodiesel. *Catalysts* 2019;9:963. <https://doi.org/10.3390/catal9110963>.
- [3] Gu Y, Son SU, Li T, Tan B. Low-Cost Hypercrosslinked Polymers by Direct Knitting Strategy for Catalytic Applications. *Adv Funct Mater* 2021;31:2008265. <https://doi.org/10.1002/adfm.202008265>.
- [4] Główniak S, Szczeńniak B, Choma J, Jaroniec M. Highly porous carbons synthesized from tannic acid via a combined mechanochemical salt-templating and mild activation strategy. *Molecules* 2021;26:1826. <https://doi.org/10.3390/molecules26071826>.
- [5] Castaldo R, Gentile G, Avella M, Carfagna C, Ambrogio V. Microporous hyper-crosslinked polystyrenes and nanocomposites with high adsorption properties: A review. *Polymers* 2017;9:651. <https://doi.org/10.3390/polym9120651>.
- [6] Ramírez-Vidal P, Suárez-García F, Canevesi RLS, Castro-Muñiz A, Gadonneix P, Paredes JI, et al. Irreversible deformation of hyper-crosslinked polymers after hydrogen adsorption. *J Colloid Interface Sci* 2022;605:513–27. <https://doi.org/10.1016/j.jcis.2021.07.104>.
- [7] Ramezanipour Penchah H, Ghaemi A, Ganadzadeh Gilani H. Benzene-Based Hyper-Cross-Linked Polymer with Enhanced Adsorption Capacity for CO₂ Capture. *Energy and Fuels* 2019;33:12578–86. <https://doi.org/10.1021/acs.energyfuels.9b03136>.
- [8] Zou L, Sun Y, Che S, Yang X, Wang X, Bosch M, et al. Porous Organic Polymers for Post-Combustion Carbon Capture. *Adv Mater* 2017;29:1700229. <https://doi.org/10.1002/adma.201700229>.
- [9] Huang N, Day G, Yang X, Drake H, Zhou HC. Engineering porous organic polymers for carbon dioxide capture. *Sci China Chem* 2017;60:1007–14. <https://doi.org/10.1007/s11426-017-9084-7>.
- [10] Cai Y, Wen X, Wang Y, Song H, Li Z, Cui Y, et al. Preparation of hyper-crosslinked polymers with hierarchical porous structure from hyperbranched polymers for adsorption of naphthalene and 1-naphthylamine. *Sep Purif Technol* 2021;266:118542. <https://doi.org/10.1016/j.seppur.2021.118542>.
- [11] Waheed A, Baig N, Ullah N, Falath W. Removal of hazardous dyes, toxic metal ions and organic pollutants from wastewater by using porous hyper-cross-linked polymeric materials: A review of recent advances. *J Environ Manage* 2021;287:112360. <https://doi.org/10.1016/j.jenvman.2021.112360>.
- [12] Xu C, Sun WZ, Qin XL, Jia YX, Yu ST, Xian M. Effective adsorption of phenolic compounds by functional group modified resins: behavior and mechanism. *Sep Sci Technol* 2019;54:467–77. <https://doi.org/10.1080/01496395.2018.1518331>.
- [13] Grätz S, Zink S, Krafczyk H, Rose M, Borchardt L. Mechanochemical synthesis of hyper-crosslinked polymers: Influences on their pore structure and adsorption behaviour for organic vapors. *Beilstein J Org Chem* 2019;15:1154–61. <https://doi.org/10.3762/bjoc.15.112>.
- [14] Masoumi H, Ghaemi A, Gilani HG. Evaluation of hyper-cross-linked polymers

- performances in the removal of hazardous heavy metal ions: A review. *Sep Purif Technol* 2021;260:118221. <https://doi.org/10.1016/j.seppur.2020.118221>.
- [15] Lee JSM, Kurihara T, Horike S. Five-Minute Mechanochemical Synthesis of Hypercrosslinked Microporous Polymers. *Chem Mater* 2020;32:7694–702. <https://doi.org/10.1021/acs.chemmater.0c01726>.
- [16] Heinicke G. Akademie Verlag, Berlin. *Acta Polym* 1985;7:400–1.
- [17] Krusenbaum A, Grätz S, Bimmermann S, Hutsch S, Borchardt L. The mechanochemical Scholl reaction as a versatile synthesis tool for the solvent-free generation of microporous polymers. *RSC Adv* 2020;10:25509–16. <https://doi.org/10.1039/d0ra05279e>.
- [18] Krusenbaum A, Geisler J, Joel F, Kraus L, Grätz S, Valentin M, et al. The mechanochemical Friedel-Crafts polymerization as a solvent-free cross-linking approach toward microporous polymers. *J Polym Sci* 2022;60:62–71. <https://doi.org/10.1002/pol.20210606>.
- [19] Ohn N, Shin J, Kim SS, Kim JG. Mechanochemical Ring-Opening Polymerization of Lactide: Liquid-Assisted Grinding for the Green Synthesis of Poly(lactic acid) with High Molecular Weight. *ChemSusChem* 2017;10:3529–33. <https://doi.org/10.1002/cssc.201700873>.
- [20] Howard JL, Cao Q, Browne DL. Mechanochemistry as an emerging tool for molecular synthesis: What can it offer? *Chem Sci* 2018;9:3080–94. <https://doi.org/10.1039/c7sc05371a>.
- [21] Julien PA, Friščić T. Methods for Monitoring Milling Reactions and Mechanistic Studies of Mechanochemistry: A Primer. *Cryst Growth Des* 2022;9:5726–54. <https://doi.org/10.1021/acs.cgd.2c00587>.
- [22] Zolriasatein A, Shokuhfar A, Safari F, Abdi N. Comparative study of SPEX and planetary milling methods for the fabrication of complex metallic alloy nanoparticles. *Micro Nano Lett* 2018;13:448–51. <https://doi.org/10.1049/mnl.2017.0608>.
- [23] Takacs L, McHenry JS. Temperature of the milling balls in shaker and planetary mills. *J Mater Sci* 2006;41:5246–9. <https://doi.org/10.1007/s10853-006-0312-4>.
- [24] Grätz S, Beyer D, Tkachova V, Hellmann S, Berger R, Feng X, et al. The mechanochemical Scholl reaction—a solvent-free and versatile graphitization tool. *Chem Comm* 2018;54:5307–10. <https://doi.org/10.1039/c8cc01993b>.
- [25] Casco ME, Badaczewski F, Grätz S, Tolosa A, Presser V, Smarsly BM, et al. Mechanochemical synthesis of porous carbon at room temperature with a highly ordered sp² microstructure. *Carbon* 2018;139:325–33. <https://doi.org/10.1016/j.carbon.2018.06.068>.
- [26] Troschke E, Grätz S, Lübken T, Borchardt L. Mechanochemical Friedel-Crafts Alkylation—A Sustainable Pathway Towards Porous Organic Polymers. *Angew Chemie* 2017;129:6963–7. <https://doi.org/10.1002/ange.201702303>.
- [27] Cook TL, Walker JA, Mack J. Scratching the catalytic surface of mechanochemistry: A multi-component CuAAC reaction using a copper reaction vial. *Green Chem* 2013;15:617–9. <https://doi.org/10.1039/c3gc36720g>.
- [28] Haley RA, Zellner AR, Krause JA, Guan H, Mack J. Nickel Catalysis in a High Speed Ball Mill: A Recyclable Mechanochemical Method for Producing Substituted Cyclooctatetraene Compounds. *ACS Sustain Chem Eng* 2016;4:2464–9. <https://doi.org/10.1021/acssuschemeng.6b00363>.

- [29] Tan L, Tan B. Hypercrosslinked porous polymer materials: design, synthesis, and applications. *Chem Soc Rev* 2017;46:3322–56. <https://doi.org/10.1039/C6CS00851H>.
- [30] Zeng H, Lu W, Hao L, Helms GL, Zhang Q, Luo Z. Adsorptive removal of p-nitrophenol from water with mechano-synthesized porous organic polymers. *New J Chem* 2018;42:20205–11. <https://doi.org/10.1039/c8nj04575e>.
- [31] Zhu X, Hua Y, Tian C, Abney CW, Zhang P, Jin T, et al. Accelerating Membrane-based CO₂ Separation by Soluble Nanoporous Polymer Networks Produced by Mechanochemical Oxidative Coupling. *Angew Chemie - Int Ed* 2018;57:2816–21. <https://doi.org/10.1002/anie.201710420>.
- [32] Zhu X, Tian C, Jin T, Browning KL, Sacci RL, Veith GM, et al. Solid-State Synthesis of Conjugated Nanoporous Polycarbazoles. *ACS Macro Lett* 2017;6:1056–9. <https://doi.org/10.1021/acsmacrolett.7b00480>.
- [33] Grätz S, Wolfrum B, Borchardt L. Mechanochemical Suzuki polycondensation-from linear to hyperbranched polyphenylenes. *Green Chem* 2017;19:2973–9. <https://doi.org/10.1039/c7gc00693d>.
- [34] Rey-Raap N, Calvo EG, Bermúdez JM, Cameán I, García AB, Menéndez JA, et al. An electrical conductivity translator for carbons. *Meas J Int Meas Confed* 2014;56:215–8. <https://doi.org/10.1016/j.measurement.2014.07.003>.
- [35] Chen H, Fan J, Fu Y, Do-Thanh CL, Suo X, Wang T, et al. Benzene Ring Knitting Achieved by Ambient-Temperature Dehalogenation via Mechanochemical Ullmann-Type Reductive Coupling. *Adv Mater* 2021;33:2008685. <https://doi.org/10.1002/adma.202008685>.
- [36] Burton TF, Pinaud J, Pétry N, Lamaty F, Giani O. Simple and Rapid Mechanochemical Synthesis of Lactide and 3S-(Isobutyl)morpholine-2,5-dione-Based Random Copolymers Using DBU and Thiourea. *ACS Macro Lett* 2021;10:1454–9. <https://doi.org/10.1021/acsmacrolett.1c00617>.
- [37] Grätz S, Oltermann M, Troschke E, Paasch S, Krause S, Brunner E, et al. Solvent-free synthesis of a porous thiophene polymer by mechanochemical oxidative polymerization. *J Mater Chem A* 2018;6:21901–5. <https://doi.org/10.1039/c8ta03684e>.
- [38] Lee GS, Lee W, Lee S, Do T, Do J, Lim J. Mechanochemical Ring-Opening Metathesis Polymerization: Development, Scope, and Mechano-Only Copolymer Synthesis. *ChemRxiv*. Cambridge: Cambridge Open Engage; 2021; This content is a preprint and has not been peer-reviewed. <https://doi.org/10.26434/chemrxiv-2021-jh72b>.
- [39] Grätz S, Borchardt L. Mechanochemical polymerization-controlling a polycondensation reaction between a diamine and a dialdehyde in a ball mill. *RSC Adv* 2016;6:64799–802. <https://doi.org/10.1039/c6ra15677k>.
- [40] Ravnsbæk JB, Swager TM. Mechanochemical Synthesis of Poly(phenylene vinylenes). *ACS Macro Lett* 2014;3:305–9. <https://doi.org/10.1021/mz500098r>.
- [41] Zhang P, Jiang X, Wana S, Dai S. Advancing Polymers of Intrinsic Microporosity by Mechanochemistry. *J Mater Chem A* 2015;3:6739–41. <https://doi.org/10.1039/C4TA07196D>.
- [42] Ohn N, Kim JG. Mechanochemical Post-Polymerization Modification: Solvent-Free Solid-State Synthesis of Functional Polymers. *ACS Macro Lett* 2018;7:561–5. <https://doi.org/10.1021/acsmacrolett.8b00171>.
- [43] Di Nardo T, Hadad C, Nguyen Van Nhien A, Moores A. Synthesis of high molecular weight chitosan from chitin by mechanochemistry and aging. *Green Chem*

- 2019;21:3276–85. <https://doi.org/10.1039/c9gc00304e>.
- [44] Pedrazzo AR, Cecone C, Trotta F, Zanetti M. Mechanochemical synthesis of β -Cyclodextrin Polymers Based on Natural Deep Eutectic Solvents. *ACS Sustain Chem Eng* 2021;9:14881–14889. <https://doi.org/10.1021/acssuschemeng.1c04988>.
- [45] Malca MY, Ferko PO, Friščić T, Moores A. Solid-state mechanochemical ω -functionalization of poly(ethylene glycol). *Beilstein J Org Chem* 2017;13:1963–8. <https://doi.org/10.3762/bjoc.13.191>.
- [46] Posudievsky OY, Kozarenko OA. Effect of monomer/oxidant mole ratio on polymerization mechanism, conductivity and spectral characteristics of mechanochemically prepared polypyrrole. *Polym Chem* 2011;2:216–20. <https://doi.org/10.1039/c0py00212g>.
- [47] Jiang JX, Cooper AI. Microporous Organic Polymers: Design, Synthesis, and Function. In: Schröder M, editor. *Functional Metal-Organic Frameworks: Gas Storage, Separation and Catalysis*. Topics in Current Chemistry. Berlin, Germany: Springer; 2009, p. 1–33. https://doi.org/10.1007/128_2009_5.
- [48] Luo D, Li M, Ma Q, Wen G, Dou H, Ren B, Liu Y, Wang X, Shui L, Chen Z. Porous organic polymers for Li-chemistry-based batteries: functionalities and characterization studies. *Chem Soc Rev* 2022;51: 2917–38. <https://doi.org/10.1039/D1CS01014J>.
- [49] Biswal BP, Chandra S, Kandambeth S, Lukose B, Heine T, Banerjee R. Mechanochemical Synthesis of Chemically Stable Isoreticular Covalent Organic Frameworks. *J Am Chem Soc* 2013;135:5328–31. <https://doi.org/10.1021/ja4017842>.
- [50] Das G, Shinde DB, Kandambeth S, Biswal BP, Banerjee R. Mechanochemical synthesis of imine, β -ketoenamine, and hydrogen-bonded imine-linked covalent organic frameworks using liquid-assisted grinding. *Chem Comm* 2014;50:12615. <https://doi.org/10.1039/c4cc03389b>.
- [51] Emmerling ST, Germann LS, Julien PA, Moudrakovski I, Etter M, Friščić T, Dinnebier RE, Lotsch BV. *In situ* monitoring of mechanochemical covalent organic framework formation reveals templating effect of liquid additive. *Chem* 2021;7:1639–52. <https://doi.org/10.1016/j.chempr.2021.04.012>.
- [52] Ardila-Fierro KJ, Hernández JG. Sustainability Assessment of Mechanochemistry by Using the Twelve Principles of Green Chemistry. *ChemSusChem* 2021;14:2145–62. <https://doi.org/10.1002/cssc.202100478>.
- [53] Lau CH, Lu T, Sun S, Chen X, Carta M, Dawson DM. Continuous flow knitting of a triptycene hypercrosslinked polymer. *Chem Comm* 2019;55:8571–74. <https://doi.org/10.1039/C9CC03731D>.
- [54] Prince L, Guggenberger P, Santini E, Kleitz F, Woodward RT. Metal-Free Hyper-Cross-Linked Polymers from Benzyl Methyl Ethers: A Route to Polymerization Catalyst Recycling. *Macromolecules* 2021;54:9217–22. <https://doi.org/10.1021/acs.macromol.1c01332>.
- [55] Du J, Ouyang H, Tan B. Porous Organic Polymers for Catalytic Conversion of Carbon Dioxide. *Chem – An Asian J* 2021;16:3833–50. <https://doi.org/10.1002/asia.202100991>.
- [56] Valverde-González A, Iglesias M, Maya EM. Metal Catalysis with Knitting Aryl Polymers: Design, Catalytic Applications, and Future Trends. *Chem Mater* 2021;33:6616–39. <https://doi.org/10.1021/acs.chemmater.1c01569>.
- [57] Gao F, Bai R, Li M, Gu Y. Dipolar HCP materials as alternatives to DMF solvent for azide-based synthesis. *Green Chem* 2021;23:7499–505.

<https://doi.org/10.1039/d1gc02002a>.

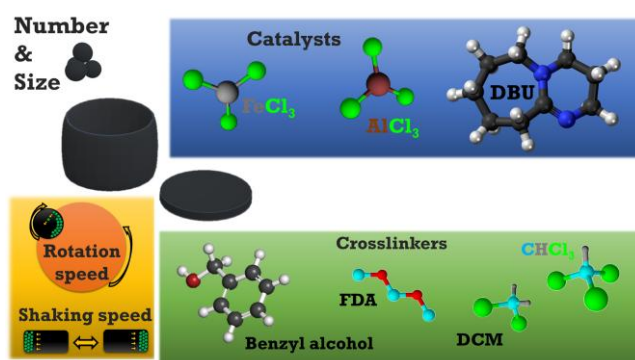
- [58] Guo S, Zhang H, Chen Y, Liu Z, Yu B, Zhao Y, et al. Visible-Light-Driven Photoreduction of CO₂ to CH₄ over N,O,P-Containing Covalent Organic Polymer Submicrospheres. *ACS Catal* 2018;8:4576–81. <https://doi.org/10.1021/acscatal.8b00989>.
- [59] Wang L, Wang R, Zhang X, Mu J, Zhou Z, Su Z. Improved Photoreduction of CO₂ with Water by Tuning the Valence Band of Covalent Organic Frameworks. *ChemSusChem* 2020;13:2973–80. <https://doi.org/10.1002/cssc.202000103>.
- [60] Bykov AV, Demidenko GN, Nikoshvili LZ, Sulman MG, Kiwi-Minsker L. Hydrogenation of a Benzene-Toluene Mixture Using Metal Nanoparticles Stabilized by a Hyper-Crosslinked Aromatic Polymer. *Chem Eng Technol* 2021;44:1955–61. <https://doi.org/10.1002/ceat.202100127>.
- [61] Mandal T, Mondal M, Choudhury J. Hypercrosslinked Polymer Platform-Anchored Single-Site Heterogeneous Pd-NHC Catalysts for Diverse C-H Functionalization. *Organometallics* 2021;40:2443–9. <https://doi.org/10.1021/acs.organomet.1c00182>.
- [62] Zhang Y, Liu K, Wu L, Huang H, Xu Z, Long Z, et al. POSS and imidazolium-constructed ionic porous hypercrosslinked polymers with multiple active sites for synergistic catalytic CO₂ transformation. *Dalt Trans* 2021;50:11878–88. <https://doi.org/10.1039/d1dt02067f>.
- [63] Li J, Wang X, Chen G, Li D, Zhou Y, Yang X, et al. Hypercrosslinked organic polymer based carbonaceous catalytic materials: Sulfonic acid functionality and nano-confinement effect. *Appl Catal B Environ* 2015;176–177:718–30. <https://doi.org/10.1016/j.apcatb.2015.04.054>.
- [64] Stepacheva AA, Markova ME, Monzharenko MA, Matveeva VG, Sulman MG. Polymer-based bifunctional catalysts for anthracene hydrocracking in the medium of supercritical propanol-2. *Catal Today* 2021;378:158–66. <https://doi.org/10.1016/j.cattod.2021.03.028>.
- [65] Lin H, Gao X, Yao H, Luo Q, Xiang B, Liu C, et al. Immobilization of a Pd(ii)-containing N-heterocyclic carbene ligand on porous organic polymers: efficient and recyclable catalysts for Suzuki-Miyaura reactions. *Catal Sci Technol* 2021;11:3676–80. <https://doi.org/10.1039/d1cy00021g>.
- [66] Yue C, Xing Q, Sun P, Zhao Z, Lv H, Li F. Enhancing stability by trapping palladium inside N-heterocyclic carbene-functionalized hypercrosslinked polymers for heterogeneous C-C bond formations. *Nat Commun* 2021;12:1–14. <https://doi.org/10.1038/s41467-021-22084-5>.
- [67] Liu Y, Zou C, Wang K, Bian Z, Jiang S, Zhou Y, et al. Palladium clusters on dicarboxyl-functional hypercrosslinked porous polymers for oxidative homocoupling of benzene with O₂. *Mol Catal* 2021;505:111487. <https://doi.org/10.1016/j.mcat.2021.111487>.
- [68] Shiryayeva VE, Popova TP, Korolev AA, Kanat'eva AY, Kurganov AA. Stationary Phase Based on Hypercrosslinked Polystyrene for Capillary Gas Chromatography. *Russ J Phys Chem A* 2020;94:1930–5. <https://doi.org/10.1134/S0036024420090253>.
- [69] Kanateva AY, Korolev AA, Kurganov AA. Preparation and properties of GC capillary column with hypercrosslinked stationary phase. *J Sep Sci* 2021;44:4395–401. <https://doi.org/10.1002/jssc.202100646>.
- [70] Penner NA, Nesterenko PN, Ilyin MM, Tsyurupa MP, Davankov VA. Investigation of the properties of hypercrosslinked polystyrene as a stationary phase for high-performance liquid chromatography. *Chromatographia* 1999;50:611–20. <https://doi.org/10.1007/BF02493669>.

- [71] Tsyurupa MP, Blinnikova ZK, Il'in MM, Davankov VA, Parenago OO, Pokrovskii OI, Usovich OI. Monodisperse microbeads of hypercrosslinked polystyrene for liquid and supercritical fluid chromatography. *Russ J Phys Chem* 2015;89:2064–71. <https://doi.org/10.1134/S0036024415110217>.
- [72] Grzywiński D, Szumski M, Buszewski B. Hypercrosslinked cholesterol-based polystyrene monolithic capillary columns. *J Chromatogr A* 2016;1477:11–21. <https://doi.org/10.1016/j.chroma.2016.11.023>.
- [73] Ramezanipour Penchah H, Ghaemi A, Ghanadzadeh Gilani H. Efficiency increase in hypercrosslinked polymer based on polystyrene in CO₂ adsorption process. *Polym Bull* 2022;79:3681–702. <https://doi.org/10.1007/s00289-021-03678-x>.
- [74] Castaldo R, Avolio R, Cocca M, Errico ME, Avella M, Gentile G. Amino-functionalized hyper-crosslinked resins for enhanced adsorption of carbon dioxide and polar dyes. *Chem Eng J* 2021;418:129463. <https://doi.org/10.1016/j.cej.2021.129463>.
- [75] Najafi P, Ramezanipour Penchah H, Ghaemi A. Synthesis and characterization of Benzyl chloride-based hypercrosslinked polymers and its amine-modification as an adsorbent for CO₂ capture. *Environ Technol Innov* 2021;23:101746. <https://doi.org/10.1016/j.eti.2021.101746>.
- [76] Ansari M, Hassan A, Alam A, Das N. A mesoporous polymer bearing 3D-Triptycene, –OH and azo- functionalities: Reversible and efficient capture of carbon dioxide and iodine vapor. *Microporous Mesoporous Mater* 2021;323:111242. <https://doi.org/10.1016/j.micromeso.2021.111242>.
- [77] Errahali M, Gatti G, Tei L, Paul G, Rolla GA, Canti L, Fraccarollo A, Cossi M, Comotti A, Sozzani P, Marchese L. Microporous Hyper-Cross-Linked Aromatic Polymers Designed for Methane and Carbon Dioxide Adsorption. *J Phys Chem C* 2014;118:28699–710. <https://doi.org/10.1021/jp5096695>.
- [78] Gatti G, Errahali M, Tei L, Cossi M, Marchese L. On the Gas Storage Properties of 3D Porous Carbons Derived from Hyper-Crosslinked Polymers. *Polymers* 2019;11:588. <https://doi.org/10.3390/polym11040588>.
- [79] Wood CD, Tan B, Trewin A, Su F, Rosseinsky MJ, Bradshaw D, Sun Y, Zhou L, Cooper AI. Microporous Organic Polymers for Methane Storage. *Adv Mater* 2008;20:1916–21. <https://doi.org/10.1002/adma.200702397>.
- [80] Tong W, Lv Y, Svec F. Advantage of nanoporous styrene-based monolithic structure over beads when applied for methane storage. *Appl Energy* 2016;183:1520–27. <https://doi.org/10.1016/j.apenergy.2016.09.066>.
- [81] Jia L, Niu B, Jiao J. Parameter Effects on Dynamic Adsorption of Trichloroethylene on Hypercrosslinked Polymeric Adsorbents. *J Environ Eng* 2020;146:04020082. [https://doi.org/10.1061/\(asce\)ee.1943-7870.0001759](https://doi.org/10.1061/(asce)ee.1943-7870.0001759).
- [82] Li X, Zhang L, Yang Z, Wang P, Yan Y, Ran J. Adsorption materials for volatile organic compounds (VOCs) and the key factors for VOCs adsorption process: A review. *Sep Purif Technol* 2020;235:116213. <https://doi.org/10.1016/j.seppur.2019.116213>.
- [83] Topuz F, Holtzl T, Szekely G. Scavenging organic micropollutants from water with nanofibrous hypercrosslinked cyclodextrin membranes derived from green resources. *Chem Eng J* 2021;419:129443. <https://doi.org/10.1016/j.cej.2021.129443>.
- [84] Yang S, Hou Y, Xiong S, Chen F, Jiang Y, Pan C, et al. Processable hypercrosslinked ionic networks for effective removal of methyl orange. *Sep Purif Technol* 2021;258:117986. <https://doi.org/10.1016/j.seppur.2020.117986>.

- [85] Mohamed MG, El-Mahdy AFM, Meng TS, Samy MM, Kuo SW. Multifunctional hypercrosslinked porous organic polymers based on tetraphenylethene and triphenylamine derivatives for high-performance dye adsorption and supercapacitor. *Polymers* 2020;12:2426. <https://doi.org/10.3390/polym12102426>.
- [86] Guerritore M, Castaldo R, Silvestri B, Avolio R, Cocca M, Errico ME, et al. Hypercrosslinked polymer nanocomposites containing mesoporous silica nanoparticles with enhanced adsorption towards polar dyes. *Polymers* 2020;12:1388. <https://doi.org/10.3390/polym12061388>.
- [87] Ou Q, Zhang QM, Zhu PC, Zhang QP, Cheng Z, Zhang C. Pentiptycene-based microporous polymer for removal of organic dyes from water. *Eur Polym J* 2019;120:109216. <https://doi.org/10.1016/j.eurpolymj.2019.109216>.
- [88] Anito DA, Wang TX, Liu ZW, Ding X, Han BH. Iminodiacetic acid-functionalized porous polymer for removal of toxic metal ions from water. *J Hazard Mater* 2020;400:123188. <https://doi.org/10.1016/j.jhazmat.2020.123188>.
- [89] Wu Z, Wei W, Ma J, Luo J, Zhou Y, Zhou Z, et al. Adsorption of Iodine on Adamantane-Based Covalent Organic Frameworks. *ChemistrySelect* 2021;6:10141–8. <https://doi.org/10.1002/slct.202102656>.
- [90] Li B, Yang X, Xia L, Majeed MI, Tan B. Hollow microporous organic capsules. *Sci Rep* 2013;3:2128. <https://doi.org/10.1038/srep02128>.
- [91] Rahnema Haratbar P, Ghaemi A, Nasiri M. Potential of hypercrosslinked microporous polymer based on carbazole networks for Pb(II) ions removal from aqueous solutions. *Environ Sci Pollut Res* 2022;29:15040–56. <https://doi.org/10.1007/s11356-021-16603-6>.
- [92] Liao G, Zhong L, Cheung CS, Du C, Wu J, Du W, et al. Direct synthesis of hypercrosslinked microporous poly(para-methoxystyrene) for removal of iron(III) ion from aqueous solution. *Microporous Mesoporous Mater* 2020;307:110469. <https://doi.org/10.1016/j.micromeso.2020.110469>.
- [93] Radford DC, Yang J, Doan MC, Li L, Dixon AS, Owen SC, et al. Multivalent HER2-binding polymer conjugates facilitate rapid endocytosis and enhance intracellular drug delivery. *J Control Release* 2020;319:285–99. <https://doi.org/10.1016/j.jconrel.2019.12.049>.
- [94] Singh P, Ren X, He Y, Wu L, Wang C, Li H, et al. Fabrication of β -cyclodextrin and sialic acid copolymer by single pot reaction to site specific drug delivery. *Arab J Chem* 2020;13:1397–405. <https://doi.org/10.1016/j.arabjc.2017.11.011>.
- [95] Osmani RA, Kulkarni P, Manjunatha S, Vaghela R, Bhosale R. Cyclodextrin nanosponge-based systems in drug delivery and nanotherapeutics: Current progress and future prospects. In: Grumezescu AM, editor. *Organic Materials as Smart Nanocarriers for Drug Delivery*. Norwich, NY: William Andrew; 2018, p. 659–717. <https://doi.org/10.1016/B978-0-12-813663-8.00016-6>.
- [96] Riyaz Ali M. Osmani, Umme Hani, Rohit R. Bhosale, Parthasarathi K. Kulkarni SS. Nanosponge Carriers- An Archetype Swing in Cancer Therapy: A Comprehensive Review. *Curr Drug Targets* 2017;18:108–18. <https://doi.org/10.2174/1389450116666151001105449>.
- [97] Ali M. Osmani R, R. Bhosale R, Hani U, Vaghela R, K. Kulkarni P. Cyclodextrin Based Nanosponges: Impending Carters in Drug Delivery and Nanotherapeutics. *Curr Drug Ther* 2015;10:3–19. <https://doi.org/10.2174/157488551001150825095513>.
- [98] Swaminathan S, Vavia PR, Trotta F, Cavalli R. Nanosponges encapsulating dexamethasone for ocular delivery: Formulation design, physicochemical

- characterization, safety and corneal permeability assessment. *J Biomed Nanotechnol* 2013;9:998–1007. <https://doi.org/10.1166/jbn.2013.1594>.
- [99] Tejashri G, Amrita B, Darshana J. Cyclodextrin based nanosponges for pharmaceutical use: A review. *Acta Pharm* 2013;63:335–58. <https://doi.org/10.2478/acph-2013-0021>.
- [100] Meng QB, Weber J. Lignin-based microporous materials as selective adsorbents for carbon dioxide separation. *ChemSusChem* 2014;7:3312–8. <https://doi.org/10.1002/cssc.201402879>.
- [101] Liu N, Chen J, Wu Z, Zhan P, Zhang L, Wei Q, Wang F, Shao L. Construction of Microporous Lignin-Based Hypercross-Linked Polymers with High Surface Areas for Enhanced Iodine Capture. *ACS Appl Polym Mater* 2021;3:2178–88. <https://doi.org/10.1021/acsapm.1c00139>.
- [102] Ansari M, Hassan A, Alam A, Das N. A mesoporous polymer bearing 3D-Triptycene, –OH and azo- functionalities: Reversible and efficient capture of carbon dioxide and iodine vapor. *Micropor Mesopor Mater* 2021;323:111242. <https://doi.org/10.1016/j.micromeso.2021.111242>.
- [103] Shao L, Liu N, Wang L, Sang Y, Wan H, Zhan P, Zhang L, Huang J, Chen J. Facile preparation of oxygen-rich porous polymer microspheres from lignin-derived phenols for selective CO₂ adsorption and iodine vapor capture. *Chemosphere* 2022;288:132499. <https://doi.org/10.1016/j.chemosphere.2021.132499>.
- [104] Liu Z, Liu H, Wang Y, Yu H, Wang J. Preparation of hypercrosslinked polymers with cashew nut shell liquid for removal of volatile organic compounds. *Polym Eng Sci* 2022;62:1823–32. <https://doi.org/10.1002/pen.25967>.
- [105] Ratvijitvech T. Bio-inspired Catechol-based Hypercrosslinked Polymer for Iron (Fe) Removal from Water. *J Polym Environ* 2020;28:2211–8. <https://doi.org/10.1007/s10924-020-01766-z>.
- [106] Ratvijitvech T, Pombejra SN. Antibacterial efficiency of microporous hypercrosslinked polymer conjugated with biosynthesized silver nanoparticles from *Aspergillus niger*. *Mater Today Commun* 2021;28:102617. <https://doi.org/10.1016/j.mtcomm.2021.102617>.
- [107] Kekevi B, Mert EH. Preparation of hypercrosslinked PolyHIPEs by using a bio-derived monomer. *Eur Polym J* 2021;152:110474. <https://doi.org/10.1016/j.eurpolymj.2021.110474>.
- [108] Zhou L, Chai K, Yao X, Ji H. Enhanced recovery of acetophenone and 1-phenylethanol from petrochemical effluent by highly porous starch-based hypercrosslinked polymers. *Chem Eng J* 2021;418:129351. <https://doi.org/10.1016/j.cej.2021.129351>.
- [109] Yuan W, Zhou L, Zhang Z, Ying Y, Fan W, Chai K, et al. Synergistic dual-functionalities of starch-grafted-styrene hydrophilic porous resin for efficiently removing bisphenols from wastewater. *Chem Eng J* 2022;429:132350. <https://doi.org/10.1016/j.cej.2021.132350>.

TOC

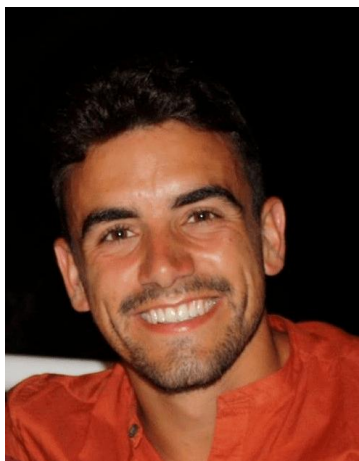


Synopsis

Critical review on mechanosynthesis of hyper-crosslinked polymers, including the most recent applications and substitution of petro- by bio- precursors.

Biographies and photographs

Antonio M. Borrero-López



Antonio María Borrero-López completed a degree in Chemical Engineering at the University of Huelva (Spain) and later received his PhD degree from the University of Huelva in 2021, with the thesis entitled “Development of new lignocellulosic-based thickening agents for biodegradable oleogel formulations with several industrial applications”. This thesis has been awarded the Best 2021–2022 Doctoral Thesis in the branch of Engineering and Architecture of the University of Huelva, and in the 2022 Occidental Andalusia Territory Section of the Spanish Royal Society of Chemistry. He has also received an honourable mention at the Annual European Rheology Conference 2022 (AERC 2022). After his PhD, he has been working as a postdoc at the Institut Jean Lamour, University of Lorraine (France), where new greener approaches for the performance of bio-based materials are being targeted. He has participated in a total of eight research projects, including the European Project UCGWATERplus, which aims to remediate waters polluted with organic and inorganic contaminants by the formulation of different products via the valorisation of the residues from underground coal gasification and other processes.

Alain Celzard



Alain Celzard graduated in chemical physics in 1992 and obtained his PhD in materials science in 1995 in Nancy (France). Since 2005, he has been a full professor at the engineering school ENSTIB (Epinal). In 2010, he was appointed junior member of the Institut Universitaire de France, and then senior member in 2022. His scientific interests focus on disordered, porous and related materials, ranging from nanoporous composites and adsorbents to macroporous solid foams for catalytic, environmental, energy or electromagnetic applications.

Vanessa Fierro



Vanessa Fierro pursued doctoral research at the Institute of Carbochemistry (ICB-CSIC) and obtained her doctorate at the University of Zaragoza (Spain). After having worked for several years as a researcher at IFP Energies Nouvelles (IFPEN) and at the Institute for Research on Catalysis and the Environment (IRCE) in Lyon (France) then at the School of Chemical Engineering in Tarragona (Spain), she is a CNRS Research Professor and a member of one of the technical groups of the Research Fund for Coal and Steel (RFCS). She currently works at the Jean Lamour Institute (France), a joint University of Lorraine-CNRS laboratory, where she leads the research team on bio-sourced materials. She received the Charles E. Pettinos Prize from the American Carbon Society in 2019 and the CNRS Silver Medal in 2020.